

Optimal intervention strategies to mitigate the COVID-19 pandemic effects

Andreas Kasis*, Stelios Timotheou, Nima Monshizadeh and Marios Polycarpou

Abstract

Governments across the world are currently facing the task of selecting suitable intervention strategies to cope with the effects of the COVID-19 pandemic. This is a highly challenging task, since harsh measures may result in economic collapse while a relaxed strategy might lead to a high death toll. Motivated by this, we consider the problem of forming intervention strategies to mitigate the impact of the COVID-19 pandemic that optimize the trade-off between the number of deceases and the socio-economic costs. We demonstrate that the healthcare capacity and the testing rate highly affect the optimal intervention strategies. Moreover, we propose an approach that enables practical strategies, with a small number of policies and policy changes, that are close to optimal. In particular, we provide tools to decide which policies should be implemented and when should a government change to a different policy. Finally, we consider how the presented results are affected by uncertainty in the initial reproduction number and infection fatality rate and demonstrate that parametric uncertainty has a more substantial effect when stricter strategies are adopted.

1 Introduction

A novel coronavirus was first reported in Wuhan, China in December 2019 [1]. The virus, now known as SARS-COV-2 [2], spread rapidly through China and the rest of the world causing the COVID-19 disease, being officially declared a pandemic by the World Health Organization (WHO) on March 17th, 2020. Since the outbreak of the COVID-19 pandemic, the world has been facing an unprecedented human tragedy along with fears of economic devastation. As a result, more than 90 million infected cases and 2 million deaths have been reported to this date (January 19, 2021). To cope with the effects of the virus, governments across the world have implemented a range of non-pharmaceutical interventions such as closing schools, banning public events and imposing social distancing, self-isolation and lockdown policies. Although such interventions may curtail the infection rate of the disease and hence the spread of the virus [3], [4], they impose an enormous economic effect. According to the International Monetary Fund [5], the economic impact of the pandemic is expected to cause the steepest worldwide recession in over 40 years and result in a loss of more than 5% of the GDP in the developed world. Hence, although a combination of social distancing and lockdown policies may be effective in containing the virus, it might be highly costly in terms of economical impact, which naturally makes government decision making a multi-objective problem.

Mathematical models are fundamental to describe the dynamic evolution of pandemics and to form effective policies to mitigate their impact. A seminal study in this area is [6], which describes the widely used susceptible - infected - recovered (SIR) model. A comprehensive review of epidemiology models can be found in [7]. Such models enable the study of the progression of various diseases over time, and facilitate the characterization of their asymptotic behaviour and dependence on model parameters. Recently, there have been various approaches to model the progression of the COVID-19 outbreak. A common approach is to apply different extensions to the SIR model, e.g. [8]. In addition, a more involved compartmental model has been developed in [9], offering larger modelling flexibility compared to simpler models. Furthermore, [10] developed an extended model which took into account the regional heterogeneity of the pandemic.

Two important parameters in the study of epidemic progression are the basic reproduction number and the infection fatality rate. The former is interpreted as the number of new people that the average person transmits the disease to while the latter enables an estimate of the fatalities resulting from the disease. The initial reproduction number, i.e. the basic reproduction number at the onset of the disease, which we

Andreas Kasis, Stelios Timotheou and Marios Polycarpou are with the KIOS Research and Innovation Center of Excellence and the Department of Electrical and Computer Engineering, University of Cyprus, Cyprus; e-mails: kasis.andreas@ucy.ac.cy, timotheou.stelios@ucy.ac.cy, mpolycar@ucy.ac.cy

Nima Monshizadeh is with the Engineering and Technology Institute, University of Groningen, Nijenborgh 4, 9747AG, Groningen, The Netherlands. email: n.monshizadeh@rug.nl

denote by \bar{R}_0 , is also of particular importance to accurately model the disease progression and in deciding the extend of government policies. However, there is significant uncertainty in estimating these parameters, as demonstrated via numerous studies that estimate \bar{R}_0 using statistical data from different countries [11], [12], [13], and various studies that have reported different infection fatality rates [14], [15], [16]. Hence, it is important to consider the effect of parametric uncertainty in forming effective government strategies.

Contribution

This study uses tools from optimal control theory to address the problem of forming a practical and efficient government intervention strategy that limits the number of fatalities due to the COVID-19 pandemic with a low social and economic cost until a vaccine is fully deployed.

In particular, we consider a controlled SIDARE (Susceptible, Infected undetected, infected Detected, Acutely symptomatic - threatened, Recovered, deceased - Extinct) model that takes into account the effect of government intervention policies. The considered model enables the integration of features such as the impact of the available healthcare capacity and testing rate. The contribution of this study is summarized as follows:

- (i) **Fatalities vs economics cost.** We present the relation between the number of fatalities and cost of optimal government intervention, and study how this relation is affected by the amount of testing and the capacity of the healthcare system to treat patients. We demonstrate the effect of these parameters in the decrease rate of the pandemic and the resulting cost associated with the optimal intervention strategy. In addition, for a range of adopted decrease tolerance levels, we provide insights on the shape of the optimal intervention strategy and its dependence on the adopted test policy.
- (ii) **Which policies and when.** We consider the fact that a government can only implement a limited number of policies and policy changes over the time span of the pandemic, due to practicality and implementability reasons and to avoid the social fatigue resulting from frequent changes in policy. Our approach provides tools to decide which policies should be implemented and when should a government change to a different policy. We demonstrate that a small number of policies and policy changes yields a close to optimal government strategy. In particular, our results suggest that the additional cost incurred from implementing 4 policies and 6 policy changes is less than 1% compared to the optimal continuously changing strategy.
- (iii) **Impact of uncertainty.** We consider the impact of uncertainty in the value of the initial basic reproduction number \bar{R}_0 and the infection fatality rate on the decrease rates resulting from optimal government strategies associated with particular decrease tolerance levels. We demonstrate that parametric uncertainty has a larger impact when stricter government policies, associated with lower decrease tolerances, are adopted.

2 Results

2.1 Problem description

To study the progression of the pandemic, we consider a controlled SIDARE (Susceptible, Infected undetected, infected Detected, Acutely symptomatic - threatened, Recovered, deceased - Extinct) model (see Fig. 1), where the effects of the healthcare capacity limit and non-pharmaceutical government interventions on the mortality and infection rates are taken into account. A full mathematical description of the controlled SIDARE model and explanations on its components are provided in Section 4. Note that the terms threatened and acutely symptomatic, as well as deceased and extinct are used interchangeably. In addition, we form a multi-objective optimization problem whose cost function consists of three components: (i) the socio-economic cost of government intervention, (ii) the cost associated with hospitalization and medical care of the acutely symptomatic population and (iii) a cost proportional to the portion of deceased population. We seek intervention strategies that minimize the aforementioned cost function. We then investigate how such strategies can be obtained with a limited number of distinct policies and policy changes in the described optimization problem. Further motivation and details concerning the mathematical formulation of the optimization problem is provided in Section 4, while our approach to solve it is detailed in the Appendix.

2.2 Deceased population vs. cost of government intervention

In this section we study the problem of forming an optimal government strategy and its dependence on selected parameters. In particular, we consider the impact of (i) the healthcare capacity limit, (ii) the testing rate and (iii) the cost emphasis on the acutely symptomatic and deceased population, on the optimal intervention

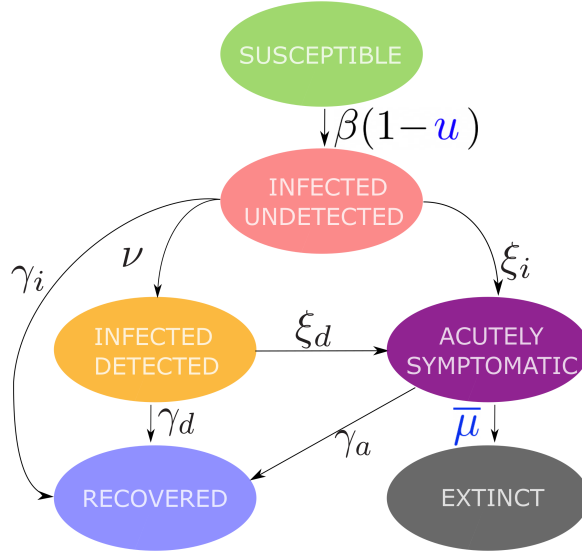


Figure 1: The controlled SIDARE model. Schematic representation of the controlled SIDARE model, used to describe the evolution of the COVID-19 pandemic. The model splits the population into Susceptible, Infected undetected, infected Detected, Acutely symptomatic - threatened, Recovered and deceased - Extinct. Model parameters $\beta, \xi_i, \xi_d, \nu, \gamma_i, \gamma_d$ and γ_a describe the transition rates between the states. The effect of government interventions is described by u which limits the rate of infection. The rate at which the acutely symptomatic population decreases is described by $\bar{\mu}$, which depends on the healthcare system capacity.

strategy and the resulting portion of deceased population. Figure 2 depicts the relation between the portion of deceases and the optimal cost of government intervention, resulting from solving the considered optimization problem (described in equation (4) in Section 4), for a range of cases for testing rate, healthcare capacity and emphasis on the acutely symptomatic and deceased population. It should be noted that all costs presented in Fig. 2 are normalised using as basis the cost of the optimal government strategy with no testing resulting to 0.01% deceases.

In particular, we considered the cases of (i) limited capacity, where two-thirds of the current healthcare capacity is used for COVID-19 patients, (ii) full capacity, where the total capacity is used and (iii) extended capacity, where the total capacity is increased by one third due to government investment and is available for COVID-19 patients. In addition, we considered the cases where (I) no testing, (II) slow testing and (III) fast testing policies are implemented. Finally, we consider three different cases for the cost emphasis on acutely symptomatic population corresponding to no emphasis (**a**), low emphasis (**b**) and high emphasis (**c**). In addition, a broad range of cost weights associated with the deceased population was considered in each case, with aim to provide a rich set of policy options. Note that a zero cost policy is only demonstrated in Fig. 2 (**a**) since having a non-zero emphasis on the acutely symptomatic population necessarily results in an optimal intervention strategy with a non-zero cost. The exact values used to produce the results presented in Fig. 2 are provided in Section 4.

From Fig. 2 we deduce the following:

- (i) The healthcare system capacity significantly affects the portion of deceased population, particularly when a low cost (Cost < 50%) strategy with no testing is implemented. This is particularly reflected in Fig. 2 (**a**) which demonstrates that increasing the available healthcare capacity from the limited level to the extended level results in up to a 50% decrease in deceases.
- (ii) When high cost government intervention strategies are adopted (Cost > 60%), then the amount of threatened population never exceeds the healthcare capacity limit and hence its value does not affect the decease rate. The latter is demonstrated from the fact that there is no shaded regions in most scenarios depicted in Fig. 2 (**b,c**).
- (iii) Increasing the amount of testing enables significantly fewer deaths for the same government intervention cost. This is reflected in Fig. 2 (**a**), which demonstrates that slow testing approximately halves the portion of deceased when compared to no testing, when a low intensity government strategy (Cost < 50%) is adopted. In addition, fast testing results in approximately half the deceases compared to slow testing and enables low cost strategies (Cost < 15%). It should be noted though that, although fast testing policies enable a reduction in costs and decease rates, they may not always be feasible since they require sufficient resources in terms of testing equipment and trained personnel.

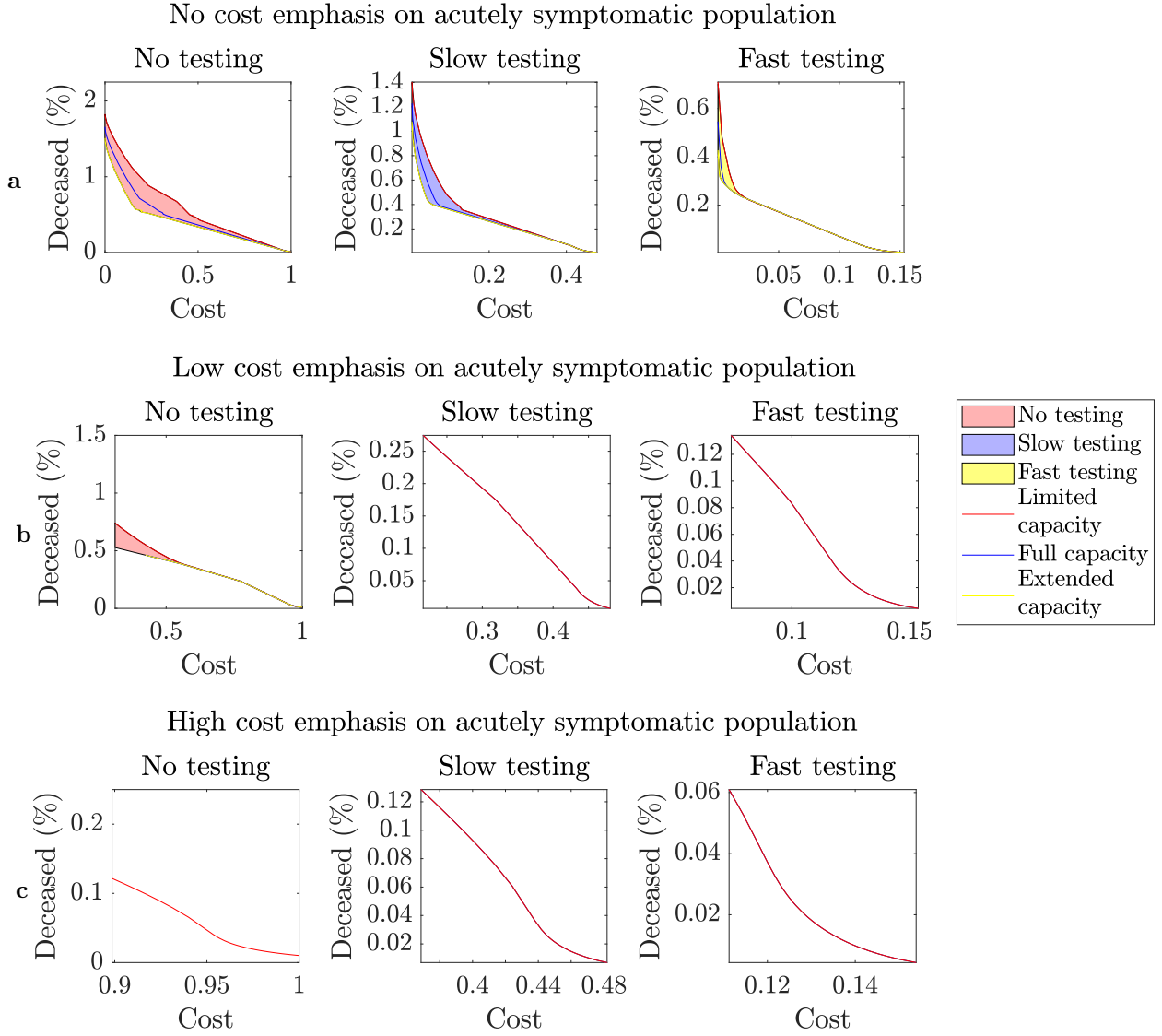


Figure 2: Deceased population vs. cost. Proportion of deceased population versus cost of optimal government intervention when the available healthcare capacity for COVID-19 patients is limited (red), full (blue), and extended (yellow) and when no testing (left), slow testing (center) and fast testing (right) policies are adopted. In addition, we present the cases where no emphasis (a), low emphasis (b) and high emphasis (c) is given to the cost associated with the acutely symptomatic population. When identical relations are obtained for different healthcare capacity levels, as for example in (c), then only the lowest capacity is presented. Shaded regions show the ranges of the relations between deceased population percentage and cost of government interaction when the healthcare capacity is between the limited and extended levels. All presented costs are normalised using as basis the cost of the optimal government strategy with no testing resulting to 0.01% deceases.

(iv) When a decrease tolerance is set, a faster testing policy enables a less intense government strategy, and hence a lower government intervention cost. For example, when a 0.1% decrease tolerance is considered, a no testing policy requires a cost of more than 90%, while slow and fast testing policies yield the same amount of deceases with costs of less than 40% and 10% respectively.

2.3 Government intervention strategies

Using the findings depicted in Fig. 2, we aimed to draw efficient intervention strategies that restrict the portion of the deceased population to specific tolerated amounts with the minimum cost. The selected portions of decrease tolerances where 1%, 0.1% and 0.01%. The approach to obtain the optimal intervention strategies is described in the appendix. The corresponding intervention strategies for each decrease tolerance level and (i) no testing, (ii) slow testing, and (iii) fast testing policy levels are depicted in Fig. 3 (a,b,c, left). Note that a fast testing policy yielded less than 1% deceases for any intervention strategy. Figure 3 depicts the intensity of optimal government intervention strategies (left) and the resulting portion of deceased (right) for each decrease tolerance level. It demonstrates the impact of testing availability in designing intervention

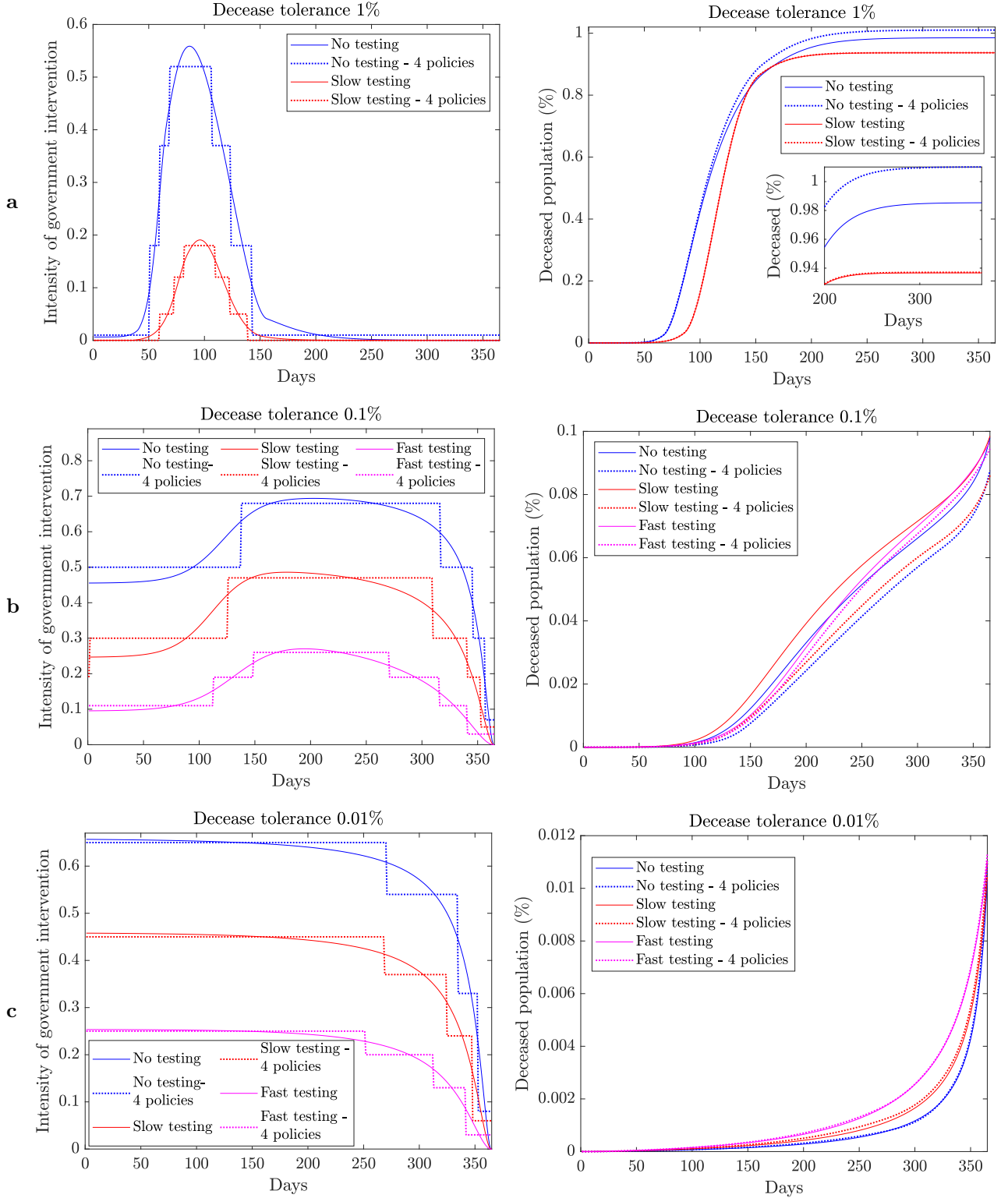


Figure 3: Optimal intervention strategies and deceased population. Optimal government intervention strategy (left) and proportion of deceased population (right) versus time for government strategies with (a) 1% decrease tolerance, (b) 0.1% decrease tolerance and (c) 0.01% decrease tolerance when (i) no testing (blue), (ii) slow testing (red) and (iii) fast testing (magenta) policies are adopted. The intensity of government intervention strategies correspond to the strictness of government policies, where 0 corresponds to no interventions and 1 to the strictest possible intervention (e.g. a full scale lockdown). The approach to obtain the optimal continuous strategy is explained in the appendix. Dotted plots correspond to optimized discrete implementations of the selected strategies by allowing a maximum of 4 policy levels and 6 policy changes. The distinct policy levels and the times where the policy was changed were selected in an optimized way, as described in Section 4 and the Appendix. Implementations with 7 and 10 policy levels and 12 and 18 policy changes are presented in the Appendix.

strategies associated with selected decrease tolerances.

The intensity of government intervention is modelled in Section 4 with a parameter u (see equation (3) in

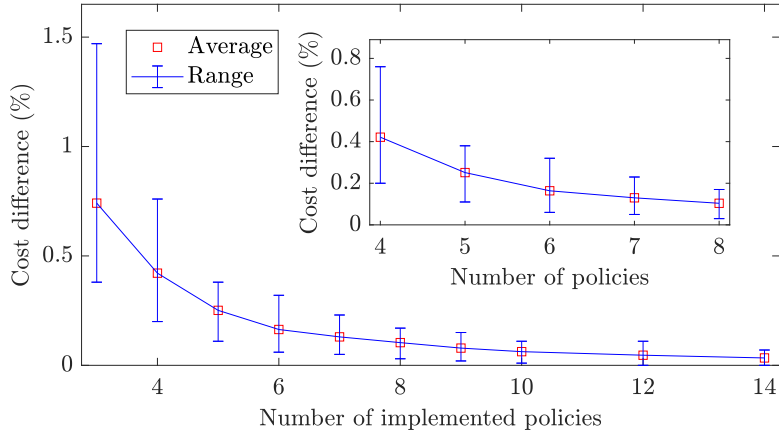


Figure 4: Additional cost from implementing a limited number of policies. Implementing a limited number of policies results in increased costs compared to the optimal continuously changing intervention strategy. This figure depicts the average and range of the percentage differences between the costs of the continuous strategies presented in Fig. 3 and strategies with a small number of policies, for different numbers of allowed distinct implemented policies. In each case, the number of allowed policy changes was twice the number of the implemented policies minus two. The boxed plot focuses on implementing between 4 and 8 distinct policies and demonstrates that 4 policies result in a cost difference of less than 1% in all cases.

Section 4 and Fig. 1), where a value of $u = 0$ corresponds to no government interventions and $u = 1$ to the strictest intervention policy (e.g. a full scale lockdown). Note that forming actual government strategies using the provided values of u , is a nontrivial task. This problem is equivalent to obtaining the basic reproduction number resulting from different intervention policies, which has been considered in [17]. For example, from [17] it can be deduced that for Italy, a school closure policy results to $u = 0.02$ while a lockdown policy to $u = 0.8$. Motivated by this, we consider any policy with $u > 0.6$ as a *very high* intensity policy. In addition, policies with $u \in [0, 0.2]$, $u \in [0.2, 0.4]$ and $u \in [0.4, 0.6]$ are referred to as *low*, *medium* and *high* intensity policies respectively.

From Fig. 3 (a), it follows that adopting a high intensity intervention strategy ($u > 0.5$) for a period of approximately 50 days is required to limit the deceases to 1% when no testing is performed. Interestingly, a slow testing policy allows a similar portion of deceased with a government strategy of about 3 times lower intensity. In addition, Fig. 3 (b) demonstrates that a 0.1% decease tolerance requires intervention strategies ranging from high to very high ($u \in [0.5, 0.7]$), medium to high ($u \in [0.25, 0.50]$), and low to medium ($u \in [0.10, 0.25]$) intensities when no, slow and fast testing policies are adopted. Furthermore, Fig. 3 (c) shows that a decease tolerance of 0.01% requires very slowly changing strategies of very high ($u \approx 0.65$), high ($u \approx 0.45$) and medium ($u \approx 0.25$) intensity when no, slow and fast testing policies are respectively adopted.

2.4 Implementing a limited number of policies and policy changes

An implementable government strategy should only have a limited number of distinct policies. In addition, frequent changes in the intervention strategy may result in social fatigue and confusion, decreasing the receptiveness of the population to the policy instructions. The policies that follow by discretizing the continuous strategies described in the previous section are depicted in Fig. 3 with dotted plots. The approach to obtain optimized strategies with a small number of policies and policy changes is described in the appendix. Figure 3 demonstrates that implementing 4 policies and allowing a maximum of 6 changes among them results in almost identical levels of decease rates compared to the continuously changing strategies. Hence, a close to optimal government response may be obtained with a relatively small number of distinct policies.

Implementing an optimal strategy with a limited number of policies and policy changes results in an increased cost compared to the optimal continuously changing strategy. The cost differences for discrete implementations of the strategies presented in Fig. 3 are depicted in Fig. 4, where a broad range of allowed number of policies is considered. For all cases the number of allowed policy changes was twice the number of implemented policies minus two. From Fig. 4, it follows that as the number of policies grows, the percentage cost difference decreases. Furthermore, as follows from the boxed plot within Fig. 4, it can be seen that a low cost difference can be obtained with a small number of policies. In particular, adopting 4 or more intervention policies allowed a cost difference of less than 1%. The latter demonstrates the effectiveness of implementing a small number of policies and policy changes.

Hence, a small number of policies and policy changes suffices for a close to optimal government response, while at the same time resolves issues of implementability and social fatigue.

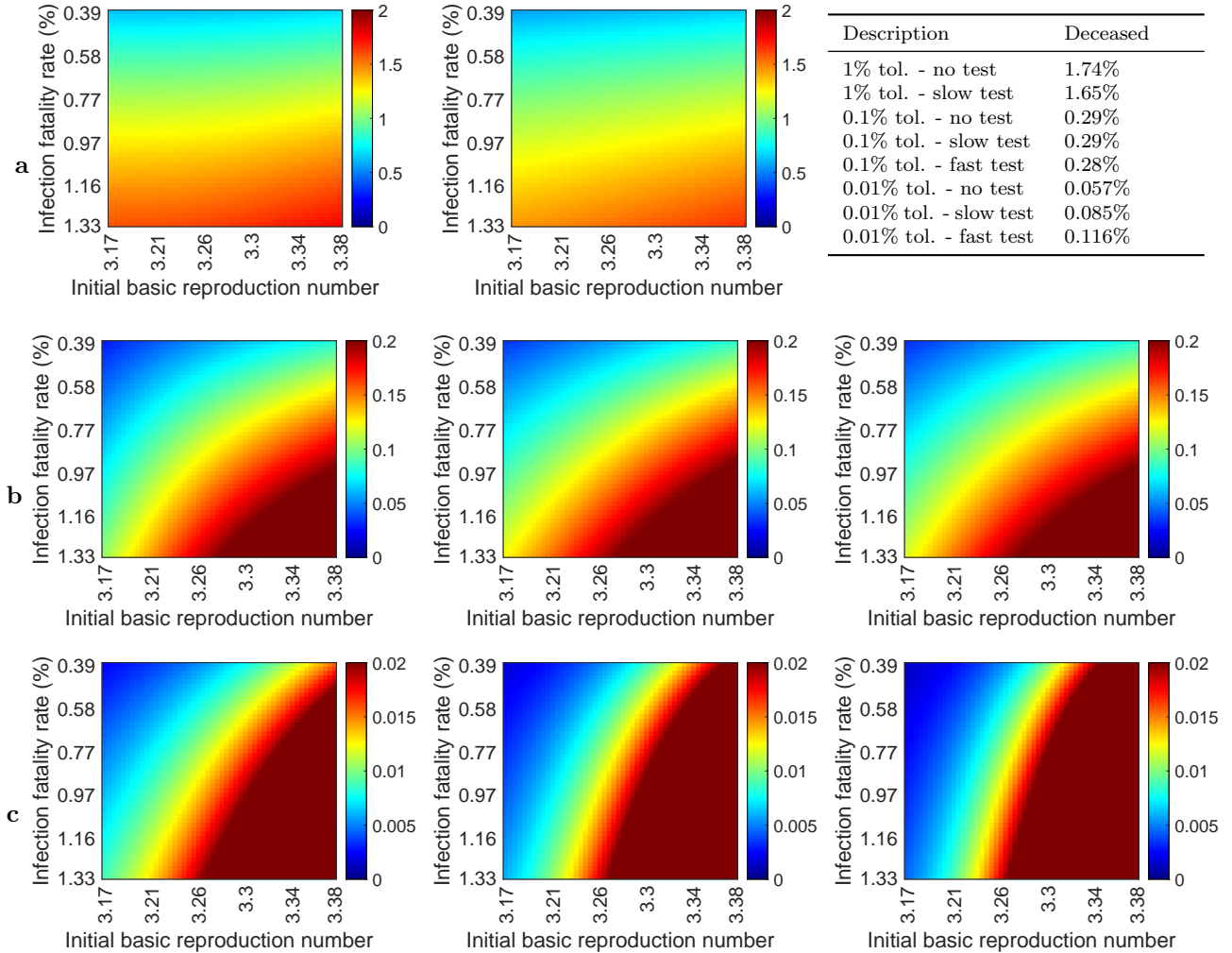


Figure 5: Effect of uncertainty in the initial reproduction and infection fatality rates. Portion of deceased for $\bar{R}_0 \in [3.17, 3.38]$ and infection fatality rate ranging between 0.39% and 1.33% associated with decrease tolerances of 1% (a), 0.1% (b) and 0.01% (c) when no (left) slow (center) and fast (right) testing policies are implemented. Fast testing always limits the decreases to less than 1% and hence there is no corresponding case. The table on (a) reports the worst case portion of deceased associated with each strategy, obtained at the maximum considered values of \bar{R}_0 and the infection fatality rate. The values were acquired by applying in each case the optimal continuous government intervention strategy obtained with $\bar{R}_0 = 3.27$ and infection fatality rate of 0.66%. Dark red and dark blue colours correspond to aggregate decreases that are at least twice and less than half the adopted tolerance levels. Additional results that demonstrate the impact of parametric uncertainty in forming effective government mitigation strategies are provided in the Appendix.

2.5 Effect of parametric uncertainty

The design of optimal control strategies relies on the use of mathematical models. Therefore, a critical aspect in designing government mitigation strategies is their dependence on parametric uncertainty, i.e. the extend of the effect of inaccurately estimating model parameters. In this section, we consider how the uncertainty in the value of the initial basic reproduction number \bar{R}_0 and the infection fatality rate affect the amount of decreases resulting from the strategies presented in the previous section.

In particular, we considered the effect on the aggregate decreases when the value of \bar{R}_0 ranges between 3.17 and 3.38 and when the infection fatality rate ranges between 0.39% and 1.33%, which correspond to 95% confidence intervals, as reported in [12] and [14] respectively.

Figure 5 demonstrates the effect of parametric uncertainty on the portion of deceased resulting from each of the 8 considered government intervention strategies presented in Fig. 3, i.e. it depicts the portion of deceased from implementing the selected strategies when \bar{R}_0 and the infection fatality rate have been imprecisely estimated. Figure 5 demonstrates that the level of adopted decrease tolerance is crucial when it comes to the effect of model uncertainty in the decrease rate.

In particular, when a 1% decrease tolerance level is adopted, the obtained policy enabled a moderate percentage increase in the total decreases, resulting to 1.75% decreases in a worst case scenario, as demonstrated in Fig. 5 (a). When the decrease tolerance level was decreased to 0.1%, then parametric uncertainty could

result in up to 0.29% decreases, i.e. about 3 times higher, as demonstrated in Fig. 5 (b) and the table in Fig. 5 (a). Finally, when a requirement for decrease tolerance level of 0.01% was imposed, then the considered uncertainty could result in up to 11.6 times higher values, as depicted in Fig. 5 (c) and the table in Fig. 5 (a). These show that parametric uncertainty should also be taken into account in forming government policies, particularly when the adopted policies are stricter, i.e. when a low decrease tolerance level is imposed.

3 Discussion

Following the COVID-19 outbreak, governments across the world have adopted strict intervention policies to contain the pandemic. However, the high economic costs resulting from these policies have spurred debates on the necessity of the measures and on how these could be relaxed without risking a new wave of infections. Recently, several approaches have been proposed to control the spread of the COVID-19 pandemic. In particular, optimal intervention strategies that simultaneously minimize the number of fatalities and the economic costs are presented in [18] and [19]. A similar problem has been considered in [20], which in addition investigated model predictive control approaches. Moreover, [21] and [22] explored the use of on-off policies to mitigate the effects of the pandemic, proposing control strategies that alternate between no measure and full measure policies. Furthermore, [10] considered regional instead of national interventions to alleviate the effects of the COVID-19 pandemic. In addition, [23] considered the problem of selecting the optimal lockdown portion that jointly minimizes the number of fatalities of the COVID-19 pandemic and the economic costs associated with the proposed policy by considering an adapted SIR model. A similar problem has been studied in [24], which in addition considered the effect of imposing different policies to different age groups.

An important missing aspect that we consider in this study is the fact that governments can only impose a limited amount of intervention policies, for practicality and implementability issues and to reduce the social fatigue resulting from frequently changing policies. We demonstrate that a small number of distinct policies and policy changes yields a close to optimal government strategy. In particular, our results suggest that the additional cost incurred from implementing 4 policies and 6 policy changes is less than 1% compared to the optimal continuously changing strategy. Using tools from optimal control theory, we provide an approach, analytically described in the appendix (see Section B), which allows to select in an optimized fashion, which policies should be implemented and when should a government switch to a different policy. Our approach can be easily applied to different types of models and cost functions, which might give emphasis to other aspects of the pandemic.

A further contribution of this paper is the study of the uncertainty in the parameters associated with the initial reproduction number and the infection fatality rate. Our results suggest that parametric uncertainty has a more significant effect when stricter government policies, aiming for lower decrease rates, are adopted.

4 Methods

We consider a SIDARE model, which is a variation of the SIR model, to describe the evolution of the COVID-19 pandemic, where the population is divided in six categories: (i) Susceptible to be infected, (ii) Infected but undetected, (iii) infected and Detected, (iv) Acutely symptomatic - threatened, (v) Recovered and (vi) Extinct - deceased. Note that we use the terms threatened and acutely symptomatic, as well as deceased and extinct interchangeably.

The dynamics of the SIDARE model are given by

$$\dot{s} = -\beta si, \tag{1a}$$

$$\dot{i} = \beta si - \gamma_i i - \xi_i i - \nu i, \tag{1b}$$

$$\dot{d} = \nu i - \gamma_d d - \xi_d d, \tag{1c}$$

$$\dot{a} = \xi_i i + \xi_d d - \gamma_a a - \mu a, \tag{1d}$$

$$\dot{r} = \gamma_i i + \gamma_d d + \gamma_a a, \tag{1e}$$

$$\dot{e} = \mu a, \tag{1f}$$

$$s(0) = s_0, i(0) = i_0, d(0) = d_0, a(0) = a_0, r(0) = r_0, e(0) = e_0, \tag{1g}$$

where $s, i, d, a, r, e \in [0, 1]$ are the states of the system describing the portions of susceptible, infected - undetected, infected - detected, threatened, recovered and deceased population respectively. Moreover, $s_0, i_0, d_0, a_0, r_0, e_0 \in [0, 1]$ denote the initial values for s, i, d, a, r, e respectively. The model parameters are briefly summarized below:

- β describes the infection rate for susceptible individuals.

- γ_i, γ_d and γ_a describe the recovery rates for infected undetected, infected detected and threatened individuals.
- ν denotes the rate of detection of infected individuals, associated with the adopted level of testing.
- ξ_i and ξ_d describe the rates at which infected undetected and infected detected individuals become acutely symptomatic.
- μ describes the mortality rate of the disease, i.e. the rate at which acutely symptomatic individuals decrease.

Note that all model parameters are assumed non-negative and constant. The SIDARE model is based on the following assumptions:

(i) Those recovered are no longer susceptible to the disease.

(ii) The considered population is constant, i.e. no births or deaths not attributed to COVID-19 are taken into account.

(iii) The considered country (or region) is isolated, i.e. no imported cases are taken into account.

(iv) Infected individuals that are detected are assumed to be quarantined, i.e. they do not contribute to new infections, something justified by existing practices.

(v) Infected individuals become acutely symptomatic before they decrease.

(vi) Acutely symptomatic individuals require hospitalization since they are considered threatened for decrease.

The assumption of constant population suggests that the states satisfy $s + i + d + a + r + e = 1$ at all times and hence that one state is redundant since it can be described by the remaining states at all times. In the analysis below, we select r to be the redundant state, satisfying $r = 1 - s - i - d - a - e$.

4.1 Impact of healthcare capacity on mortality rate

An important aspect that we consider is the impact of the healthcare system capacity on the mortality rate. It is evident that when the healthcare capacity is exceeded, then the mortality rate of the population increases. The latter is modelled in equation (2), which suggests that the mortality rate depends on the portion of acutely symptomatic population by the relation

$$\bar{\mu}(a) = \begin{cases} \mu a, & \text{if } a \leq \bar{h}, \\ \mu \bar{h} + \hat{\mu}(a - \bar{h}), & \text{if } a > \bar{h}, \end{cases} \quad (2)$$

where the function $\bar{\mu} : [0, 1] \rightarrow \mathbb{R}_+$ describes the mortality of the acutely symptomatic population. The values of μ and $\hat{\mu}$ satisfy $\mu < \hat{\mu}$ and correspond to the mortality rates when the healthcare system satisfies the demand and when the healthcare capacity is exceeded by much. This means that when the infected population increases, the mortality rate tends to $\hat{\mu}$. In addition, the value of \bar{h} describes the existing healthcare capacity. Note that for simplicity we assume a constant value of \bar{h} , although its value could rise in the future due to a possible increase in the healthcare system capacity.

4.2 Modelling government interventions on the SIDARE model

To account for the effect of the government actions to mitigate the spread of the pandemic, we introduce an intervention input u to the SIDARE model. Its value affects the infection rate of the disease, β , resulting in a slower spread. The controlled SIDARE model follows from equation (1) when β is replaced by $\beta(1 - u)$ and in addition includes the healthcare capacity impact on the mortality rate, described by equation (2). Its dynamics are given by

$$\dot{s} = -\beta si(1 - u), \quad (3a)$$

$$\dot{i} = \beta si(1 - u) - \gamma_i i - \xi_i i - \nu i, \quad (3b)$$

$$\dot{d} = \nu i - \gamma_d d - \xi_d d, \quad (3c)$$

$$\dot{a} = \xi_i i + \xi_d d - \gamma_a a - \bar{\mu}(a), \quad (3d)$$

$$\dot{e} = \bar{\mu}(a), \quad (3e)$$

$$s(0) = s_0, i(0) = i_0, d(0) = d_0, a(0) = a_0, e(0) = e_0, \quad (3f)$$

$$s + i + d + a + r + e = 1, \quad (3g)$$

where $u \in \mathcal{U} = [0, \bar{u}]$ and $\bar{u} \leq 1$ is a positive constant that denotes the maximum value that the intervention policy u is allowed to take. Since government actions should only aid in curtailing the effects of the pandemic, u is not allowed to take negative values. The dynamics of the controlled SIDARE model are depicted in Fig. 1.

The value of $u(t)$ corresponds to the government intervention policy at time t , with higher values of u corresponding to stricter intervention policies. For example, when a government does not take any action, then $u = 0$ and when a government takes the strictest possible measures, e.g. when implementing a full scale lockdown, then $u = \bar{u}$.

4.3 A multi objective optimization problem

A suitable government strategy should aim to simultaneously minimize the number of fatalities and the costs associated with implementing intervention policies. The number of the aggregate fatalities during the considered period is given by $e(T)$, where the constant $T > 0$ denotes the considered timeframe.

Moreover, any policy u comes with a cost associated with the social and economic side effects from its implementation. For example, a lockdown policy has an economic cost due to the inability of a portion of the population to work and a social cost associated with restricting the population movements and interactions. In addition, we consider the cost associated with the acutely symptomatic population. The latter describes the costs resulting from people requiring additional care, including possible hospitalization. These motivate the following cost functional,

$$C(u, a) = \int_0^T \frac{1}{2} u(t)^2 dt + \theta_a \int_0^T \frac{1}{2} a(t)^2 dt,$$

where the non-negative parameter θ_a describes the weight given on the cost associated with the threatened population. The proposed cost functional sets a penalty analogous to the square of the intervention effort u , set by the government to mitigate the effects of the disease, and the square of the aggregate threatened population a . Note that a quadratic cost is considered in order to enable a close estimate to the non-linear cost effects arising from intense government strategies and from having a large portion of the population being in a threatened state.

However, there is a trade-off between minimizing the economic cost of government policies and the number of fatalities. The above motivates the following optimization problem

$$\begin{aligned} \min_{u \in \mathcal{U}} J(a, e, u) &= C(u, a) + \theta_e e(T) \\ \text{s.t.} & \quad (3), \end{aligned} \tag{4}$$

where θ_e describes the weight given to the total number of deaths in comparison with the cost associated with the threatened population and government intervention effort. The values of weight coefficients θ_e and θ_a are key to form the optimal policy. For example, if $\theta_e = \theta_a = 0$, then the focus of the government is to minimize the socio-economic cost of the intervention strategy, which trivially results to $u = 0$ for all times. On the other hand, when θ_a and θ_e are large, then the focus becomes to minimize the number of fatalities and the number of acutely symptomatic individuals, which results in a value of u that is close to \bar{u} at all times. Since there is a trade-off between these objectives, selecting suitable values for θ_e and θ_a is highly important. Furthermore, note that the relative ratio between θ_a and θ_e enables an extra degree of freedom in the choice of the optimization problem and a richer set of solutions. The approach to solve the above optimization problem, using tools from optimal control theory, is explained in the appendix (see Section B).

4.4 Implementing a limited number of policies and policy changes

A government can only implement a limited number of policies and policy changes over the time span of the pandemic, for practicality and to avoid the social fatigue resulting from frequent policy changes. To account for this, we restrict both the number of distinct implemented policies and policy changes in the previously considered optimization problem.

We denote the set of possible policies by \mathcal{U}_d , the set of distinct policies within strategy u by $\mathcal{R}(u) = \{\tilde{u} : \exists t \in [0, T] \text{ s.t. } u(t) = \tilde{u}\}$ and the set of switching instants by $\mathcal{T} = \{t \in [0, T] : \lim_{\epsilon \rightarrow 0} u(t - \epsilon) \neq \lim_{\epsilon \rightarrow 0} u(t + \epsilon)\}$. The revised problem is given by

$$\begin{aligned} \min_{u \in \mathcal{U}_d} J(a, e, u) \\ \text{s.t.} \quad (3), |\mathcal{R}(u)| \leq \hat{n}_1, |\mathcal{T}| \leq \hat{n}_2, \end{aligned} \tag{5}$$

where \hat{n}_1 and \hat{n}_2 denote the maximum number of policies that u is allowed to take from the set \mathcal{U}_d and the maximum allowed number of changes in the intervention strategy over the considered timeframe respectively. The solution approach for problem (5) is analytically described within the Appendix.

4.5 Simulated parameters

In this section, we describe and justify the parameters considered in the simulation results presented in Section 2. We use the controlled SIDARE model, described by equation (3), for our simulations, with a time horizon of $T = 365$ days. The selected initial conditions correspond to the very early stage of the disease, where 0.001%

of the population has been infected and there are no detected cases, acutely symptomatic cases, fatalities or recoveries yet. When possible, data associated with the pandemic in Italy were used for consistency.

The values of γ_i and γ_d were selected following [25], which suggests a median time of disease onset to recovery for mild cases of approximately two weeks. The value of γ_a was selected following [26], which reported a median time between hospitalization and recovery of 12.4 days. Furthermore, to select the values for ξ_i and ξ_d , we used the findings from [14] on hospitalization rate per age group and data for the Italian population age distribution [27]. In addition, for the results presented in Fig. 3–5, we considered a healthcare capacity of 333 care beds per 100,000 habitants following [28], which corresponded to the full capacity case. The maximum allowed value for u , given by \bar{u} , was selected to be 0.8 to account for the fact that complete isolation is impossible, since always some critical units will need to remain operational.

The value of β was selected following an initial basic reproduction number of approximately 3.27 as estimated in [12] and the relation $\bar{R}_0 = \beta s_0 / (\gamma_i + \xi_i + \nu)$ which is analytically shown in the appendix (see Section A), assuming $\nu = 0$ at $t = 0$ days. The value of μ was selected following a median infection fatality rate of 0.66%, as reported in [14]. We let $\hat{\mu}$, which corresponds to the fatality rate when the healthcare system capacity is overloaded, be 5 times higher than μ , motivated by the findings in [29]. In addition, the values for θ_a associated with no, low and high emphasis on acutely symptomatic population were $0, 5 \times 10^4$ and 10^5 respectively. For each case, a broad range of cost coefficients associated with the deceased population was considered, letting $\theta_e \in [0, 2.5 \times 10^4]$. The no, slow and fast testing policies corresponded to values of ν of 0, 0.05 and 0.10 respectively. Additional explanations on the simulated parameters are provided in the Appendix.

5 Conclusion

We considered the problem of forming government intervention strategies that optimize the trade-off between the number of deceases and the social and economic costs. We demonstrate the relation between the number of fatalities and cost of optimal government intervention, and how this depends on the adopted testing policy and the healthcare system capacity. Moreover, we determine that a small number of policies and policy changes suffices for a close to optimal intervention strategy. In particular, our results suggest that implementing 5 policies and 8 policy changes enables a cost difference of less than 1% compared to a continuously changing strategy. Finally, we considered the impact of uncertainty in the initial reproduction number and infection fatality rate and demonstrated that its effect is more severe when intense government strategies are implemented.

Appendix

This appendix describes the methodology used to obtain the main results of the paper. In particular, we provide analytical results that describe the behaviour of the SIDARE model and explain how we obtain the optimal government intervention strategy for given parameters. Moreover, we present a detailed algorithm that yields an optimized strategy with a limited number of policies and policy changes. Furthermore, we provide additional details regarding the presented numerical simulations and include extra simulation results with aim to enable additional clarity and intuition on the presented findings.

Notation

The set of natural numbers is denoted by \mathbb{N} . The projection of a scalar x to a set X is denoted by $[x]_X = \arg \min_{y \in X} |y - x|$. The interior of a set X is denoted by X° . The cardinality of a discrete set Σ is denoted by $|\Sigma|$. A monotonically increasing (respectively decreasing) function $f : \mathbb{R} \rightarrow \mathbb{R}$ satisfies $f(x) \leq f(y)$ (respectively $f(x) \geq f(y)$) for all x, y such that $x \leq y$. The notation $x \geq 0$ implies that all elements of vector x are non-negative. In addition, we use \dot{x} to denote the time derivative of a signal x .

A Analysis of the SIDARE model

A.1 Analytical results for the SIDARE model

The SIDARE model, given by equation (1), is a bilinear system with six states. Below, we demonstrate that all states in equation (1) take non-negative values, provided that the initial conditions are non-negative, which is clearly in line with intuition.

Lemma 1. *Consider equation (1) and let all states take non-negative values at $t = 0$. Then, all states take non-negative values for all times.*

Proof of Lemma 1: If all states takes non-negative values at the initial conditions, then from equation (1a), it follows that s can not take negative values by continuity and the fact that $\dot{s} = 0$ when $s = 0$. It then follows that i is also non-negative from s being non-negative and equation (1b). Similar arguments hold for states d and a , i.e. the non-negativity of i and (i, d) respectively and the dynamics in equations (1c)–(1d) suffice so that d and a are non-negative. Finally, the non-negativity of (i, d, a) implies that $\dot{r} \geq 0$ and $\dot{e} \geq 0$ from equations (1e) and (1f) respectively and hence that r and e are also non-negative. ■

It should also be noted that from equations (1a), (1e), and (1f) and Lemma 1, it follows that the state s is monotonically decreasing and the states r and e are monotonically increasing.

The following lemma characterises the equilibria of equation (1). Note that we let $x = (s, i, d, a, r, e)$ for convenience. In addition, we denote an equilibrium of (1) by $x^* = (s^*, i^*, d^*, a^*, r^*, e^*)$.

Lemma 2. *The set of equilibria of (1) is given by $S = \{x^* : i^* = d^* = a^* = 0\}$.*

Proof of Lemma 2: Any equilibrium of equation (1) should satisfy $s^* i^* = 0$ from equation (1a). This suggests from equation (1b) that $i^* = 0$, which in turn suggests from equation (1c) that $d^* = 0$. An equilibrium with $i^* = d^* = 0$ also satisfies $a^* = 0$ from equation (1d). Moreover, consider any point in the state space of equation (1) with $i = d = a = 0$. This point is necessarily an equilibrium since all equations (1a)–(1f) are zero. ■

The following proposition enables to define the basic reproduction number \bar{R}_0 in terms of model parameters. Note that the definitions of stable and unstable equilibria follow from [30, Definition 4.1]. Within Proposition 1, we make use of the set $X_{\geq 0} = \{x : x \geq 0\}$.

Proposition 1. *Consider an equilibrium point of (1), given by $x^* = (s^*, 0, 0, 0, r^*, e^*)$ and let $x(0)$ take non-negative values. Then,*

- (i) *if $s^* < (\gamma_i + \xi_i + \nu)/\beta$, then there exists a neighbourhood Z of x^* such that solutions initiated in $Z \cap X_{\geq 0}$ asymptotically converge to an equilibrium point within Z .*
- (ii) *if $s^* > (\gamma_i + \xi_i + \nu)/\beta$, then x^* is an unstable equilibrium point.*

Proof of Proposition 1: We first prove part (i), using Lyapunov based arguments, and then part (ii).

Part (i): First note that since all states take non-negative values at $t = 0$, then they take non-negative values at all times from Lemma 1. Furthermore, from equations (1a), (1e), and (1f) it follows that the state s is monotonically decreasing and the states r and e are monotonically increasing.

For the system described by equation (1), we consider an equilibrium point x^* and the Lyapunov candidate function

$$V(x) = V_1(s, r, e) + V_2(i, d, a),$$

where

$$V_1(s, r, e) = \frac{1}{2}(s - s^*)^2 + \frac{1}{2}(r - r^*)^2 + \frac{1}{2}(e - e^*)^2,$$

and

$$V_2(i, d, a) = i + \theta_1 d + \theta_2 a,$$

where θ_1 and θ_2 are positive constants.

The dynamics of equation (1) suggest that

$$\dot{V}_1(x) = (s - s^*)(-\beta s i) + (r - r^*)(\gamma_i i + \gamma_d d + \gamma_a a) + (e - e^*)\mu a \leq 0$$

where the inequality holds since $s(t) \geq s^*$, $r(t) \leq r^*$ and $e(t) \leq e^*$ for all times since s is monotonically decreasing and r and e are monotonically increasing and all states i, d, a and parameters $\beta, \gamma_i, \gamma_d, \gamma_a$ and μ take non-negative values.

In addition, it follows that along trajectories of equation (1) it holds that

$$\dot{V}_2(x) = \beta s i - \gamma_i i - \xi_i i - \nu i + \theta_1(\nu i - \gamma_d d - \xi_d d) + \theta_2(\xi_i i + \xi_d d - \gamma_a a - \mu a).$$

Note that for solutions initiated sufficiently close to x^* it holds that $s(t) < (\gamma_i + \xi_i + \nu)/\beta$ at all times due to the monotonicity of s . Therefore, letting $\rho = (\gamma_i + \xi_i + \nu) - \beta s(0)$ it follows that $\dot{i} \leq -\rho i$ at all times and consequently

$$\dot{V}_2(x) \leq -\rho i + \theta_1(\nu i - \gamma_d d - \xi_d d) + \theta_2(\xi_i i + \xi_d d - \gamma_a a - \mu a).$$

Hence, there exist positive θ_1, θ_2 satisfying $\theta_1 \nu + \theta_2 \xi_i < \rho$ and $\theta_2 \xi < \theta_1(\gamma_d + \xi_d)$ such that

$$\dot{V} = \dot{V}_1 + \dot{V}_2 \leq -\phi_1 i - \phi_2 d - \phi_3 a \leq 0, \quad (6)$$

where ϕ_1, ϕ_2 and ϕ_3 are positive constants. Hence, there exists a compact connected set Ξ which includes x^* , given by $\Xi = \{x : V(x) \leq r\}$, for sufficiently small $r > 0$, such that solutions initiated within Ξ remain in Ξ for all times. Since r can be selected to be arbitrarily small, it follows that x^* is a stable equilibrium of (1).

LaSalle's invariance principle [30][Theorem 4.4] can now be applied on the compact and positively invariant set Ξ . This guarantees that solutions to equation (1) initiated in Ξ converge to the largest invariant set within $\Xi \cap \{x : \dot{V}(x) = 0\}$. If $\dot{V} = 0$ holds within Ξ it follows from equation (6) that $(i, d, a) = (0, 0, 0)$. The latter implies convergence of the states (s, r, e) from equations (1a) and (1e)–(1f) to the set of equilibria within Ξ .

In addition, note that if r in the definition of Ξ is selected to be sufficiently small, then Ξ contains only stable equilibria, satisfying $s^* < (\gamma_i + \xi_i + \nu)/\beta$. This allows to deduce that solutions initiated within Ξ asymptotically converge to an equilibrium point by using arguments analogous to those in [31, Prop. 4.7, Thm 4.20].

Part (ii): Consider any equilibrium x^* such that $s^* > (\gamma_i + \xi_i + \nu)/\beta$. Then, the Jacobian matrix associated with the linearisation of equation (1) at x^* is given by

$$J_{x^*} = \begin{bmatrix} 0 & -\beta s^* & 0 & 0 & 0 & 0 \\ 0 & \beta s^* - \gamma_i - \xi_i - \nu & 0 & 0 & 0 & 0 \\ 0 & \nu & -\gamma_d - \xi_d & 0 & 0 & 0 \\ 0 & \xi_i & \xi_d & -\gamma_a - \mu & 0 & 0 \\ 0 & \gamma_i & \gamma_d & \gamma_a & 0 & 0 \\ 0 & 0 & 0 & \mu & 0 & 0 \end{bmatrix}.$$

It can easily be shown that J_{x^*} has three zero eigenvalues and three more given by $-\gamma_d - \xi_d$, $-\gamma_a - \mu$ and $\beta s^* - \gamma_i - \xi_i - \nu$. When $s^* > (\gamma_i + \xi_i + \nu)/\beta$, the last eigenvalue is positive which suggests that the linearisation at x^* is unstable. ■

The value of \bar{R}_0 corresponds to the basic reproduction rate. Stability of the dynamics described by equation (1) imply a basic reproduction rate of less than or equal to 1. Hence, for the considered case it holds that $\bar{R}_0 \bar{s} = 1$. Therefore, from Proposition 1 it follows that the value of \bar{R}_0 is given by $\bar{R}_0 = 1/\bar{s} = \beta/(\gamma_i + \xi_i + \nu)$.

It should be noted that all analytical results presented above, can be trivially extended when the term μa in equations (1d) and (1f) is replaced with $\bar{\mu}(a)$.

B Optimal control methodology

In this section we present the solution approach that yields the optimal continuous strategy and optimized strategies with a limited number of policies and policy changes.

To improve the presentation of the results, we note that the states a and e are uniquely defined by the initial conditions and u , and hence a functional \mathcal{J} can be defined such that $\mathcal{J}(u) = J(a, e, u)$ for given initial conditions. Therefore, the optimization problem Problem (4) can be equivalently written as

$$\begin{aligned} & \min_{u \in \mathcal{U}} \mathcal{J}(u) \\ & \text{s.t. (3).} \end{aligned} \tag{7}$$

B.1 Solution approach

We call \hat{u} a solution to Problem (4) if $\mathcal{J}(\hat{u}) = \min_{u \in \mathcal{U}} \mathcal{J}(u) = \min_{u \in \mathcal{U}} J(a, e, u)$. We call the solution \hat{u} and the corresponding state \hat{x} an optimal pair. The existence of a solution to Problem (4) is established by the following lemma.

Lemma 3. *There exists a solution to Problem (4).*

Proof of Lemma 3: To prove Lemma 3, we apply [32, Thm. 2.1, p. 63], which provides sufficient conditions for the existence of an optimal solution to a general optimal control problem. In particular, the conditions in [32, Thm. 2.1, p. 63] are satisfied for Problem (4) since:

- (i) Equation (3) is continuously differentiable,
- (ii) there exist a feasible solution to equation (3),
- (iii) \mathcal{U} is a compact set,
- (iv) $F(t, x) = \{[-\beta si(1-u), \beta si(1-u) - \gamma_i i - \xi_i i - \nu i, \nu i - \gamma_d d - \xi_d d, \xi_i i + \xi_d d - \gamma_a a - \bar{\mu}(a), \bar{\mu}(a)]^T : u \in \mathcal{U}\}$ is convex for all $(t, s, i, d, a, e) \in [0, T] \times [0, 1]^5$.

Hence, there exists an optimal solution \hat{u} to Problem (4). ■

To obtain the optimal intervention strategy \hat{u} , it will be convenient to form the Hamiltonian for Problem (4), as below

$$H(x, u, \lambda) = \frac{1}{2}u^2 + \frac{1}{2}\theta_a a^2 + \lambda^T (f_0(x) + f_1(x)u) \tag{8}$$

where $\lambda \in \mathbb{R}^5$ is called the co-state of the system and $f_0(x)$ and $f_1(x)$ follow from equation (3) and are given¹ by

$$f_0(x) = \begin{bmatrix} -\beta si \\ \beta si - \gamma_i i - \xi_i i - \nu i \\ \nu i - \gamma_d d - \xi_d d \\ \xi_i i + \xi_d d - \gamma_a a - \bar{\mu}(a) \\ \bar{\mu}(a) \end{bmatrix}, \quad f_1(x) = \begin{bmatrix} \beta si \\ -\beta si \\ 0 \\ 0 \\ 0 \end{bmatrix}.$$

Below, we provide necessary optimality conditions for Problem (4), which are a result of Pontryagin's minimum principle.

Proposition 2. *Let (\hat{x}, \hat{u}) be a locally optimal pair to Problem (4). Then, there exists a co-state function $\hat{\lambda} : [0, T] \rightarrow \mathbb{R}^5$ such that the following conditions hold for almost all $t \in [0, T]$:*

$$\dot{\hat{\lambda}}^T = -(\hat{\lambda}^T (\nabla f_0(\hat{x}) + \nabla f_1(\hat{x})\hat{u})), \tag{9a}$$

$$\hat{\lambda}(T) = [0 \ 0 \ 0 \ 0 \ \theta_e]^T, \tag{9b}$$

$$\hat{u} = [-\hat{\lambda}^T f_1(\hat{x})]_{\mathcal{U}} \tag{9c}$$

Proof of Proposition 2: The proof follows from applying Pontryagin's minimum principle [33] in Problem (4). The principle states that for a trajectory (\hat{x}, \hat{u}) that solves Problem (4), there exists a function $\hat{\lambda} : [0, T] \rightarrow \mathbb{R}^5$ that that:

$$\dot{\hat{x}}^T = \frac{\partial H}{\partial \lambda}(\hat{x}(t), \hat{u}(t), \hat{\lambda}(t)), \quad \hat{x}(0) = x_0, \tag{10a}$$

$$\dot{\hat{\lambda}}^T = -\frac{\partial H}{\partial x}(\hat{x}(t), \hat{u}(t), \hat{\lambda}(t)), \tag{10b}$$

$$\hat{\lambda}(T) = \frac{\partial S}{\partial x}(\hat{x}(T))^T, \tag{10c}$$

$$H(\hat{x}(t), \hat{u}(t), \hat{\lambda}(t)) \leq H(\hat{x}(t), u(t), \hat{\lambda}(t)), \quad \forall u \in \mathcal{U}, \tag{10d}$$

¹Note that the state r within x does not appear in either $f_0(x)$ or $f_1(x)$. We defined f_0 and f_1 as functions of x to avoid introducing extra notation.

where the Hamiltonian H is given by equation (8) and S is associated with the final cost, and is given by $S(x) = \theta_e e$. Hence, equation (9) follows directly² from equations (8) and (10). Note that equation (9c) follows from equation (10d), which results to $\frac{\partial H}{\partial u}(\hat{x}(t), \hat{u}(t), \hat{\lambda}(t)) = 0$ when $\hat{u} \in \mathcal{U}^\circ$, i.e. when \hat{u} lies in the interior of \mathcal{U} . ■

We make use of equation (9) and the controlled SIDARE model dynamics, described by equation (3) to obtain the optimal solution to Problem (4). To tackle the challenges associated with dealing with initial and final value constraints in numerical simulations, we used an adapted forward-backward sweep method (e.g. [36, Ch. 21]).

B.2 Implementing a limited amount of policies and policy changes

An implementable government strategy requires that u takes a small number of distinct values, i.e. there exists a finite set of distinct possible intervention policies $\mathcal{U}_d = \{\tilde{u}_1, \tilde{u}_2, \dots, \tilde{u}_{\tilde{m}}\} \subset \mathcal{U}$ such that $u(t) \in \mathcal{U}_d$ for all $t \geq 0$. For notational convenience, it is assumed that $\tilde{u}_i < \tilde{u}_j$ for $i < j$. Moreover, for each strategy u , we consider the set of policy change instants $\mathcal{T} = \{t_1, t_2, \dots, t_n\}$ satisfying $0 < t_1 < t_2 < \dots < t_n < T$, where $T > 0$ denotes the considered timeframe, such that $u(t) = u_j \in \mathcal{U}_d, t \in [t_{j-1}, t_j), 1 \leq j \leq n+1$, where $t_0 = 0$ and $t_{n+1} = T$. In addition, it is assumed that $u_j \neq u_{j+1}, 1 \leq j \leq n-1$. Note that the cardinality of the set \mathcal{T} is important as it describes the amount of changes between policies. For any intervention strategy u , we let $\mathcal{R}(u) = \{\tilde{u} : \exists t \in [0, T] \text{ s.t. } u(t) = \tilde{u}\}$ satisfying $\mathcal{R}(u) \subseteq \mathcal{U}_d$ denote the set of policies within u . In addition, $|\mathcal{R}(u)|$ describes the number of distinct policies within strategy u .

Drawing a practical government intervention strategy motivates the introduction of two constraints: (i) on the number of distinct policies, so that a small set of rules is implemented by the population, (ii) on the number of policy changes, since frequent policy changes may result in social fatigue, decreasing the responsiveness of the population to the policy instructions. To account for these, we have defined the optimization problem (5), presented also below for convenience:

$$\begin{aligned} & \min_{u \in \mathcal{U}_d} J(a, e, u) \\ & \text{s.t. (3), } |\mathcal{R}(u)| \leq \hat{n}_1, |\mathcal{T}| \leq \hat{n}_2, \end{aligned}$$

where \hat{n}_1 and \hat{n}_2 respectively denote the maximum number of policies that u is allowed to take from the set \mathcal{U}_d and the maximum allowed number of changes in the intervention policy over the considered timeframe. In analogy to (7), Problem (5) can be equivalently written as

$$\begin{aligned} & \min_{u \in \mathcal{U}_d} \mathcal{J}(u) \\ & \text{s.t. (3), } |\mathcal{R}(u)| \leq \hat{n}_1, |\mathcal{T}| \leq \hat{n}_2. \end{aligned} \tag{11}$$

To solve the above problem, we make use of the solution to Problem (4), which is a continuous relaxation to Problem (5), and hence provides a lower bound to the cost of Problem (5). Our approach to obtain a solution to Problem (5) is described below:

(i) Obtain \hat{u} that solves Problem (4).

(ii) Using \hat{u} , obtain an optimized solution to Problem (5), denoted by \hat{u}_d , resulting from a local minimum cost search algorithm.

Part (i) of the above approach is explained in Section B.1 above (see also Proposition 2). Part (ii) is described in detail below.

Part (ii): The methodology in this section is split in two steps. First, we obtain a strategy that approximates \hat{u} and simultaneously satisfies the constraints of Problem (5). Using this strategy for initialization, we implement Algorithm 1 which produces the optimized policy \hat{u}_d . Note that in the presented process, it is assumed that $\hat{n}_1 > 1$ and $\hat{n}_2 \geq 1$. The case where $\hat{n}_1 = 1$ which necessarily results in $|\mathcal{T}| = \emptyset$ can be trivially solved by evaluating the costs of implementing each value of $u \in \mathcal{U}_d$.

Initialization: The first step aims to obtain an intervention strategy \bar{u}_d that approximates the continuous strategy \hat{u} and simultaneously satisfies the constraints of the problem. To obtain such strategy, we let $u_{max} = \max_{t \in [0, T]} \hat{u}$ and $u_{min} = \min_{t \in [0, T]} \hat{u}$ and define $\hat{u}_i = [u_{min} + (i-1) * (u_{max} - u_{min}) / (\hat{n}_1 - 1)]_{\mathcal{U}_d}$ and $U_s = \{\hat{u}_i : i \in \{1, \dots, \hat{n}_1\}\}$, where \hat{n}_1 is given in Problem (5). Consequently, we let $v_d(t) = \arg \min_{y \in U_s} |y - \hat{u}(t)|$ for all $t \in [0, T]$, i.e. we project the values of the continuous policy \hat{u} onto the discrete set U_s . The latter leads to $\mathcal{R}(v_d) = U_s$. Moreover, we define the set $\bar{\mathcal{T}}^i = \{t \in [0, T] : \lim_{\epsilon \rightarrow 0} v_d(t + \epsilon) \neq \lim_{\epsilon \rightarrow 0} v_d(t - \epsilon)\}$, i.e. the set of all time instants when a change occurs in the intervention policy v_d .

²Note that there is a technical issue in the definition of $\frac{\partial H}{\partial x}$ when $a = \bar{h}$ since $\frac{d\bar{\mu}(a)}{da}$ is not well defined at this point. This issue can be resolved by considering the subdifferential of $\bar{\mu}(a)$ at $a = \bar{h}$ [34], and define the solutions for x and λ in the sense of Filippov [35]. We refrain from properly defining these concepts to avoid the introduction of extensive technical notions and to keep the focus of the paper on the practical aspects of the results.

If $|\bar{\mathcal{T}}^i| \leq \hat{n}_2$, then we select $\bar{u}_d = v_d$. Otherwise, we define $|\bar{\mathcal{T}}^i|$ strategies $v_{d,j}$, such that strategy $v_{d,j}$ satisfies $v_{d,j}(t) = v_d(t), t \in [0, T] \setminus [t_j, t_{j+1})$ and $v_{d,j}(t) = v_d(t_{j-1}), t \in [t_j, t_{j+1})$, i.e. $v_{d,j}$ follows by omitting the j th switch in v_d . We then calculate the cost for each of the above policies, given by $\mathcal{J}(v_{d,j})$, and select the $q = |\bar{\mathcal{T}}^i| - \hat{n}_2$ strategies with the least cost. Finally, we neglect the switches associated with these q strategies from v_d , i.e. the q switches which individually cause the least increase in cost once removed, to construct \bar{u}_d . The latter enables the construction of \bar{u}_d which satisfies all the constraints of Problem (5).

Algorithm 1: After obtaining \bar{u}_d , as explained above, then an optimized solution \hat{u}_d is obtained from Algorithm 1, as described below. To initialise Algorithm 1, we first consider the set of switching instants for strategy \bar{u}_d , which we denote by $\bar{\mathcal{T}}$, and select a sufficiently small $\delta > 0$ which corresponds to the tolerance of Algorithm 2, implemented within Algorithm 1. In addition, the vector p , with $p \in \mathbb{N}^{|\mathcal{R}(\hat{u}_d)|}$, represents the indices of implemented policies from \mathcal{U}_d in strategy \bar{u}_d in decreasing order, i.e. $p_i = k$ means that the i th largest implemented policy is \tilde{u}_k , reminding that $\mathcal{U}_d = \{\tilde{u}_1, \tilde{u}_2, \dots, \tilde{u}_m\}$.

Algorithm 1 aims to obtain an optimized intervention strategy, denoted by \hat{u}_d , by making incremental changes in the test policy \hat{u}_t , as seen in equations (A.1.1)–(A.1.2), e.g. when $m = 1$ and $n = 1$ then Algorithm 1 replaces the largest policy within \hat{u}_t with the immediately more relaxed policy within \mathcal{U}_d , in analogy when $n = 2$ then the attempted policy is the one which is the immediately more strict. Then, Algorithm 2, described in detail below, makes use of the test policy \hat{u}_t and set of switching times \mathcal{T} and provides a new test policy with an optimized set of switching times, denoted by $\tilde{\mathcal{T}}$, and a corresponding cost, denoted by C . If C is less than the lowest cost obtained by that stage, denoted by C_m , then \hat{u}_d is updated as in equation (A.1.4.1). In addition, the supplementary variables C_m, p and $\bar{\mathcal{T}}$ are updated to facilitate the progression of the algorithm, as described in equations (A.1.4.2)–(A.1.4.4).

The convergence variable θ takes the value of 0, which imposes that a new set of iterations need to be performed for the convergence of the algorithm. If there is no improvement in C_m for all $m \in \{1, \dots, |\mathcal{R}(\hat{u}_d)|\}$ and $n \in \{1, 2\}$, then Algorithm 1 converges. Convergence of Algorithm 1 suggests that any incremental change in any of the policies within \hat{u}_t will result in a higher cost, and hence that a local minimum has been reached. For improved clarity, a flowchart of Algorithm 1 is presented in Fig. 6.

Algorithm 2: Algorithm 2 aims to obtain an optimized set of switching times, denoted by $\tilde{\mathcal{T}}$ and a corresponding intervention strategy \hat{u}_t by making use of the discrete test policy \hat{u}_t , the set of switching times \mathcal{T} and the tolerance level δ provided from Algorithm 1 for its initialization. In particular, it alters the switching times by δ in either direction, as demonstrated in equation (A.2.1) and updates \bar{u}_t as described in equations (A.2.2)–(A.2.3). Then, a new cost is calculated, based on the new strategy \bar{u}_t by implementing equation (A.2.4). If the new cost, denoted by \tilde{C} is lower than the cost obtained by policy \hat{u}_t , then the cost, the policy and the set of switching times are updated, as demonstrated in equations (A.2.5.1)–(A.2.5.3). Otherwise, the policy \bar{u}_t reverts to its previous value.

The variable ϕ serves as a convergence variable. In particular, when any iteration occurs that allows a decrease in cost then its value is set to 0, which results in a new set of iterations for $\tilde{\mathcal{T}}$. Convergence of the algorithm suggests that a local minimum of the cost C is reached, where changing any switching time in $\tilde{\mathcal{T}}$ does not result in a lower cost. For improved intuition, Fig. 7 depicts a flowchart of Algorithm 2.

Algorithm 1 creates a monotonically decreasing sequence of values for C , which is lower bounded by $C^* = \mathcal{J}(\hat{u})$, i.e. the cost associated with the optimal continuous policy obtained in part (i). Therefore, the sequence of updates in C and hence Algorithm 1 converge, as directly follows by the monotone convergence theorem (e.g. [37, Theorem 2.4.2]). A similar argument follows for the convergence of Algorithm 2.

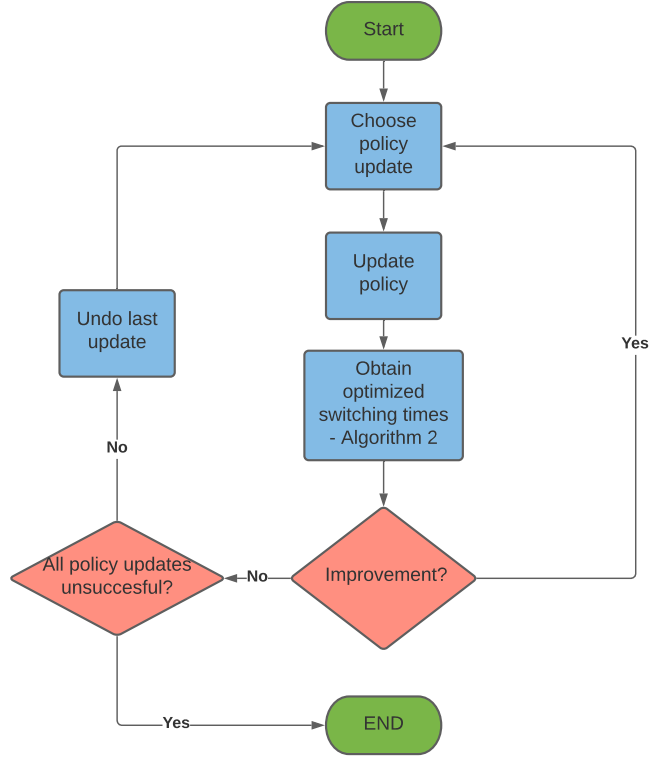


Figure 6: Flowchart for Algorithm 1.

Algorithm 1: Scheme to obtain \hat{u}_d .

Inputs: $\tilde{\mathcal{T}}, \bar{u}_d, \delta, \mathcal{U}_d, p$.

Output: \hat{u}_d .

Initialization:

$$C = \mathcal{J}(\bar{u}_d), C_m = C, \mathcal{T} = \tilde{\mathcal{T}}, \hat{u}_d = \hat{u}_t = \bar{u}_d, \theta = 0.$$

while $\theta = 0$ **do**

$\theta = 1$,

for $m = 1 : |\mathcal{R}(\hat{u}_d)|$

for $n = 1 : 2$

$$\hat{\mathcal{T}} = \{t : \hat{u}_d(t) = \tilde{u}_{p_m}\}, \quad (\text{A.1.1})$$

$$\hat{u}_t(t) = \tilde{u}_{[p_m + (-1)^n]_{[1, \bar{m}]}}, t \in \hat{\mathcal{T}}, \quad (\text{A.1.2})$$

$$[\tilde{\mathcal{T}}, \hat{u}_t, C] = \text{Algorithm 2}(\mathcal{T}, \hat{u}_t, \delta) \quad (\text{A.1.3})$$

if $C < C_m$,

$$\hat{u}_d = \hat{u}_t, \quad (\text{A.1.4.1})$$

$$C_m = C, \quad (\text{A.1.4.2})$$

$$p_m = [p_m + (-1)^n]_{[1, \bar{m}]}, \quad (\text{A.1.4.3})$$

$$\mathcal{T} = \tilde{\mathcal{T}}, \quad (\text{A.1.4.4})$$

$$\theta = 0, \quad (\text{A.1.4.5})$$

else

$$\hat{u}_t = \hat{u}_d, \quad (\text{A.1.4.6})$$

end

end

end

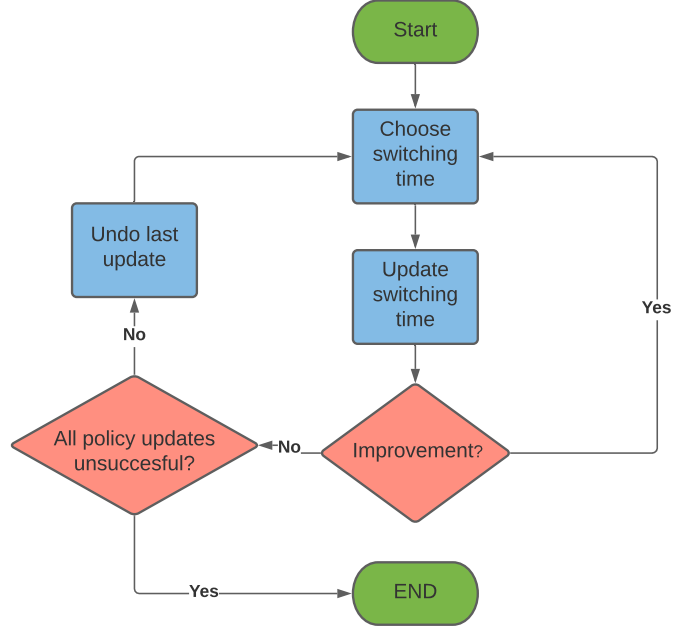


Figure 7: Flowchart for Algorithm 2.

Algorithm 2: Scheme to obtain $\tilde{\mathcal{T}}, \hat{u}_t, C$.

Inputs: $\mathcal{T}, \hat{u}_t, \delta$.

Output: $\tilde{\mathcal{T}}_i, 1 \leq i \leq |\mathcal{T}|, \hat{u}_t, C$.

Initialization:

$$C = \mathcal{J}(\hat{u}_t), \bar{u}_t = \hat{u}_t, \tilde{\mathcal{T}} = \mathcal{T}, \phi = 0, \tilde{\mathcal{T}}_0 = 0, \tilde{\mathcal{T}}_{|\mathcal{T}|+1} = T.$$

while $\phi = 0$ **do**

$\phi = 1,$

for $k = 1 : |\mathcal{T}|$

for $j = 1 : 2$

$$\hat{\delta} = \delta \times (-1)^j, \quad (\text{A.2.1})$$

$$\tilde{\mathcal{S}} = \begin{cases} [[\tilde{\mathcal{T}}_k + \hat{\delta}]_{[\tilde{\mathcal{T}}_{k-1}, \tilde{\mathcal{T}}_k]}, \tilde{\mathcal{T}}_k], & \text{if } j = 1, \\ [\tilde{\mathcal{T}}_k, [\tilde{\mathcal{T}}_k + \hat{\delta}]_{[\tilde{\mathcal{T}}_k, \tilde{\mathcal{T}}_{k+1}]}], & \text{if } j = 2, \end{cases} \quad (\text{A.2.2})$$

$$\bar{u}_t(t) = \hat{u}_t(\tilde{\mathcal{T}}_{k+1-j}), \forall t \in \tilde{\mathcal{S}}, \quad (\text{A.2.3})$$

$$\tilde{C} = \mathcal{J}(\bar{u}_t), \quad (\text{A.2.4})$$

if $\tilde{C} < C$

$$C = \tilde{C}, \quad (\text{A.2.5.1})$$

$$\hat{u}_t = \bar{u}_t, \quad (\text{A.2.5.2})$$

$$\phi = 0, \quad (\text{A.2.5.3})$$

$$\tilde{\mathcal{T}}_k = [\tilde{\mathcal{T}}_k + \hat{\delta}]_{[\tilde{\mathcal{T}}_{k-1}, \tilde{\mathcal{T}}_{k+1}]}, \quad (\text{A.2.5.4})$$

else

$$\bar{u}_t = \hat{u}_t, \quad (\text{A.2.5.5})$$

end

end

end

C Supplementary Results

In this section, we present additional results that supplement the presented findings. In particular, we present optimized strategies and the corresponding decrease rates when 4, 7 and 10 distinct policies and 6, 12 and 18 policy changes are allowed. Furthermore, we complement our results associated with the effect of parametric

uncertainty, depicted in Fig. 5, with additional results demonstrating the optimal strategies and corresponding aggregate deceases for a range of values for the infection fatality rate and initial basic reproduction number \bar{R}_0 . These results aim to provide additional intuition on the effect of parametric uncertainty in forming efficient government strategies.

C.1 Simulated parameters

The controlled SIDARE model, described by equation (3) has been used in our simulations, with a time horizon of $T = 365$ days. The selected initial conditions correspond to the very early stage of the disease, where 0.001% of the population has been infected and there are no detected cases, acutely symptomatic cases, fatalities or recoveries yet.

The values of γ_i and γ_d were selected following [25], which suggests a median time of disease onset to recovery for mild cases of approximately two weeks. The value of γ_a was selected following [26], which reported a median time between hospitalization and recovery of 12.4 days.

The value of β was selected to be 0.251, corresponding to an initial basic reproduction number $\bar{R}_0 = \beta s_0 / (\gamma_i + \xi_i + \nu)$ of approximately 3.27 following [12], and assuming $\nu = 0$ at $t = 0$ days. The value of \bar{u} , corresponding to the maximum allowed value for the input u was selected to be 0.8. Furthermore, to select the values for ξ_i and ξ_d for the case of Italy, we used the findings from [14] on hospitalization rate per age group and data for the Italian population age distribution [27]. In addition, we considered 333 care beds per 100,000 habitants following [28].

The value of μ was selected to be 0.0085, being associated with an infection fatality rate of 0.66% as reported in [14]. The latter is in agreement with various studies that report a mortality rate close or below 1% [15], [38], [16]. We let $\hat{\mu}$, which corresponds to the fatality rate when the healthcare system capacity is overloaded, be 5 times higher than μ , motivated from [29] which compared the fatality rates in two regions in Italy, Lombardy where more than 80% of the healthcare capacity was held by COVID-19 patients and Veneto where up to 40% was held, and deduced an approximate five fold increase in the mortality rate.

To facilitate the reproducibility of the results, the parameter values used in the simulations, and the justification for their selection, are reported in Table 1.

Table 1: Model parameter values

Parameter	Value	Justification
$(s_0, i_0, d_0, a_0, e_0)$	$(1 - 10^{-5}, 10^{-5}, 0, 0, 0)$	Early stage of the pandemic
γ_i, γ_d	$1/14 = 0.071$	[25]
γ_a	$1/12.4$	[26]
β	0.251	\bar{R}_0 from [12]
ξ_i, ξ_d	0.0053	[14], [27]
μ	0.0085	[14]
\bar{h}	0.0481	[28]
$\hat{\mu}$	$5 \times \mu$	[29]

C.2 Deceased population versus cost of government intervention

In Fig. 2, we associate the cost of (optimal) government intervention and the portion of deceased population when: (i) different hospital capacity rates, (ii) different testing rates and (iii) different cost emphasis levels associated with the acutely symptomatic population, are considered. Note that in each case we considered a broad range of cost weight values associated to the total number of deaths. The considered cases for hospital capacity rates, testing rates, and cost weights attributed to the acutely symptomatic cases and the total number of deaths are presented in Table 2.

Table 2: Parameters associated with the cases presented in Fig. 2.

Parameter	Symbol	Cases
Hospital capacity rate	\bar{h}	$\{222, 333, 444\} \times 10^{-5}$
Testing rate	ν	$\{0, 0.05, 0.10\}$
Cost weight for acutely symptomatic cases	θ_a	$\{0, 5 \times 10^4, 10^5\}$
Cost weight for aggregate deaths	θ_e	$[0, 2.5 \times 10^4]$

The parameters from Table 2 associated with each of the 8 intervention strategies presented in Fig. 3 are provided in Table 3 below. In all cases, the considered hospital capacity rate was 333 care beds per 100,000

habitants which corresponded to the full capacity case.

Table 3: Parameters associated with the optimal continuous strategies presented in Fig. 3.

Tolerance (%)	Testing rate	Cost weight for acutely symptomatic cases	Cost weight for aggregate deaths
1	0	0	1600
1	0.05	0	400
0.1	0	10^5	600
0.1	0.05	10^5	1000
0.1	0.10	5×10^4	1000
0.01	0	0	2.5×10^4
0.01	0.05	0	1.8×10^4
0.01	0.10	0	10^4

C.3 Implementing a limited number of policies and policy changes

In Fig. 8–15, we present the intervention strategies and corresponding aggregate deceases associated with decrease tolerances of 1%, 0.1% and 0.01%. In particular, we present the optimal continuous strategy and optimized intervention strategies with 4, 7 and 10 distinct policy levels and 6, 12 and 18 policy changes respectively. These results are associated with Fig. 3, which however includes only the case where 4 distinct policies and 6 policy changes are allowed. The results presented in Fig. 8–15 demonstrate that increasing the number of distinct policies enables a decrease response that is closer to the optimal continuous strategy, which is in agreement with intuition.

C.4 Effect of parametric uncertainty

In Fig. 16–31, we present additional results associated with the effect of uncertainty in knowledge of the initial reproduction number \bar{R}_0 and the infection fatality rate. These results aim to provide additional intuition and clarity on the presented results.

In particular, we first consider the case where the value of \bar{R}_0 ranges between 3.17 and 3.38, which corresponds to a 95% confidence interval, as reported in [12] when the infection mortality rate is 0.66%, as reported in [14]. For the considered case, we obtain the optimal strategies which correspond to each value of \bar{R}_0 for the parameters presented in Table 3, associated with the 8 continuous strategies presented in Fig. 3. The ranges of the obtained optimal intervention strategies for each of these 8 considered cases are depicted in Fig. 16–23 (left). From these figures, it follows that the uncertainty in \bar{R}_0 results in small variations in the optimal strategies when no and slow testing policies are adopted. By contrast, when fast testing policies are implemented, the impact of the uncertainty in \bar{R}_0 on the optimal strategies is more substantial.

Moreover, Fig. 16–23 (right) demonstrate the ranges of decrease rates obtained when the same 8 selected strategies are applied for $\bar{R}_0 \in [3.17, 3.38]$ when the infection mortality rate is 0.66%, i.e. they depict the decrease rates from implementing the selected strategies when the value of \bar{R}_0 has been incorrectly estimated. The effect of implementing the 8 selected strategies when in addition the infection mortality rate has been incorrectly estimated is demonstrated in Fig. 24–31, which depict the decrease rates for the considered range of values for \bar{R}_0 when the infection mortality rate is 0.39% and 1.33% respectively. These values represent the lower and upper bounds of a 95% infection mortality rate confidence interval, as reported in [14]. Figures 16–23 (right) and Fig. 24–31 demonstrate that the level of the adopted decrease tolerance is crucial when it comes to the effect of model uncertainty in the decrease rates. The latter is in agreement with the presented results, which state that parametric uncertainty has a more substantial effect when stricter government strategies, associated with lower decrease tolerances, are adopted.

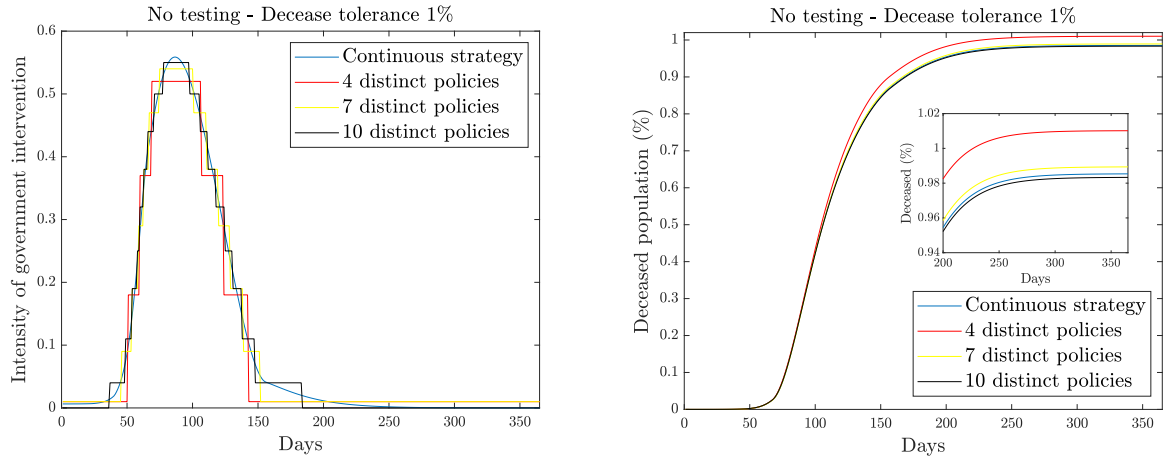


Figure 8: Intervention strategy and decrease rate, 1% decrease tolerance, no testing. Intensity of government intervention (left) and portion of deceased population (right) when no testing is performed and a decrease tolerance of 1% is adopted when (i) a continuously changing strategy is selected and (ii) discrete implementations of the selected strategy are considered, allowing 4, 7 and 10 policy levels and 6, 12 and 18 policy changes respectively.

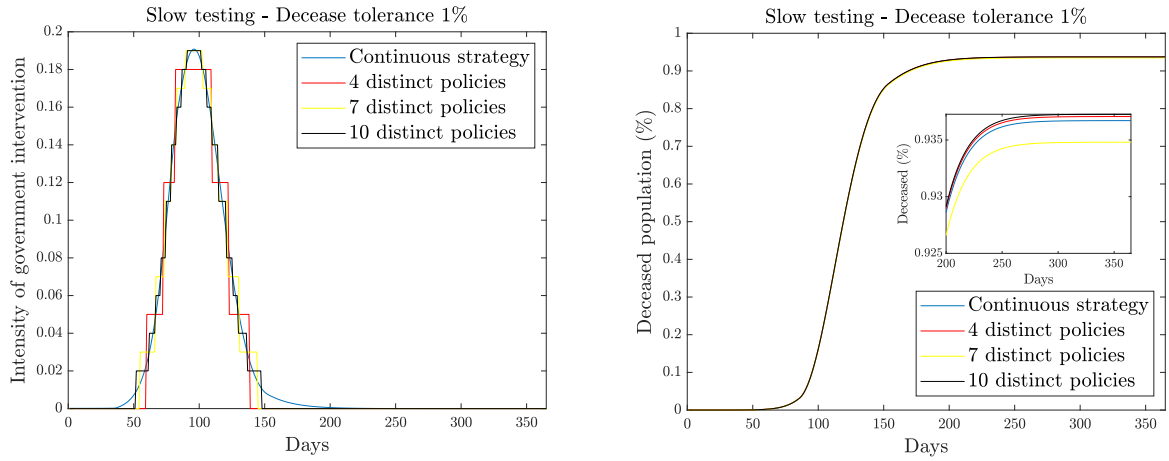


Figure 9: Intervention strategy and decrease rate, 1% decrease tolerance, slow testing. Intensity of government intervention (left) and portion of deceased population (right) when a slow testing policy and a decrease tolerance of 1% are adopted when (i) a continuously changing strategy is selected and (ii) discrete implementations of the selected strategy are considered, allowing 4, 7 and 10 policy levels and 6, 12 and 18 policy changes respectively.

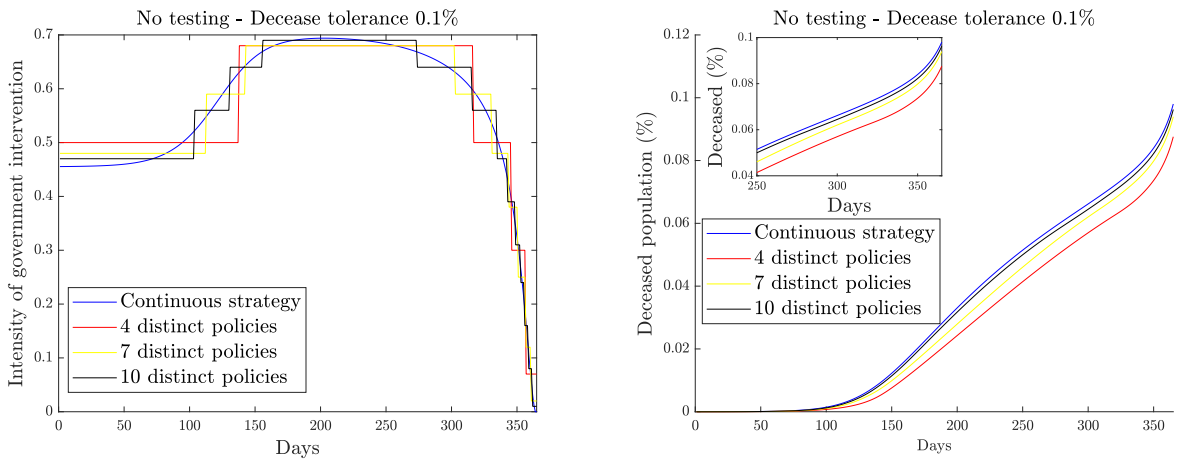


Figure 10: Intervention strategy and decrease rate, 0.1% decrease tolerance, no testing. Intensity of government intervention (left) and portion of deceased population (right) when no testing is performed and a decrease tolerance of 0.1% is adopted when (i) a continuously changing strategy is selected and (ii) discrete implementations of the selected strategy are considered, allowing 4, 7 and 10 policy levels and 6, 12 and 18 policy changes respectively.

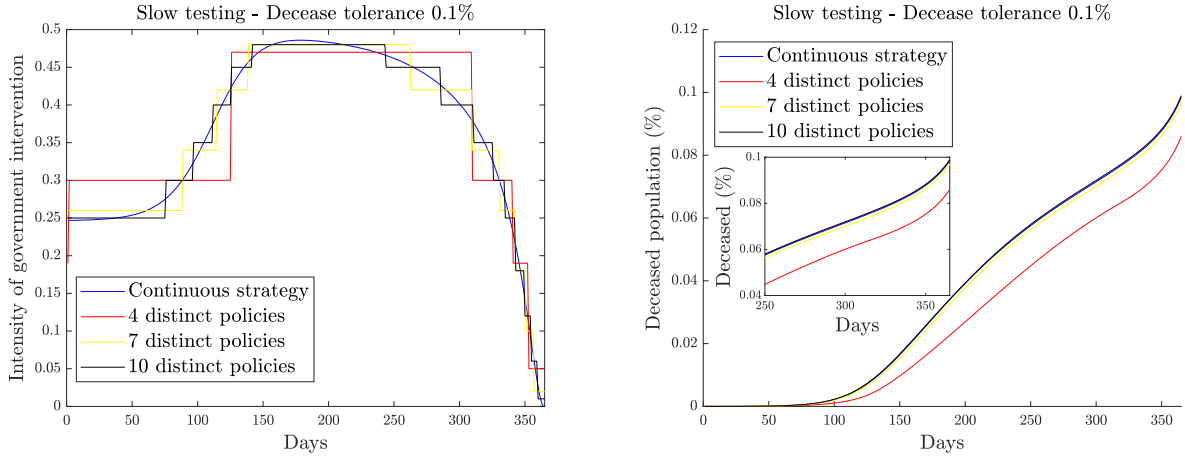


Figure 11: Intervention strategy and decrease rate, 0.1% decrease tolerance, slow testing. Intensity of government intervention (left) and portion of deceased population (right) when a slow testing policy and a decrease tolerance of 0.1% are adopted when (i) a continuously changing strategy is selected and (ii) discrete implementations of the selected strategy are considered, allowing 4, 7 and 10 policy levels and 6, 12 and 18 policy changes respectively.

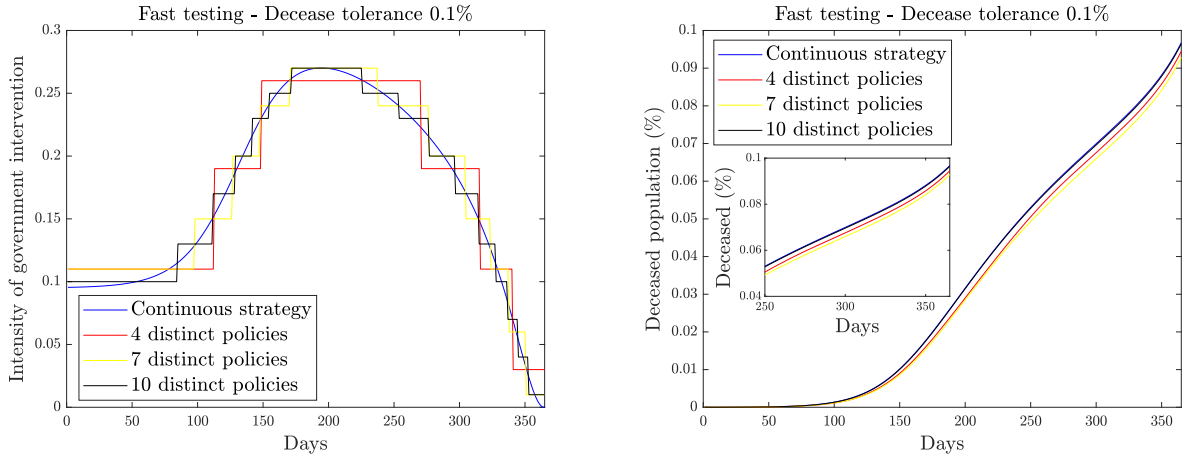


Figure 12: Intervention strategy and decrease rate, 0.1% decrease tolerance, fast testing. Intensity of government intervention (left) and portion of deceased population (right) when a fast testing policy and a decrease tolerance of 0.1% are adopted when (i) a continuously changing strategy is selected and (ii) discrete implementations of the selected strategy are considered, allowing 4, 7 and 10 policy levels and 6, 12 and 18 policy changes respectively.

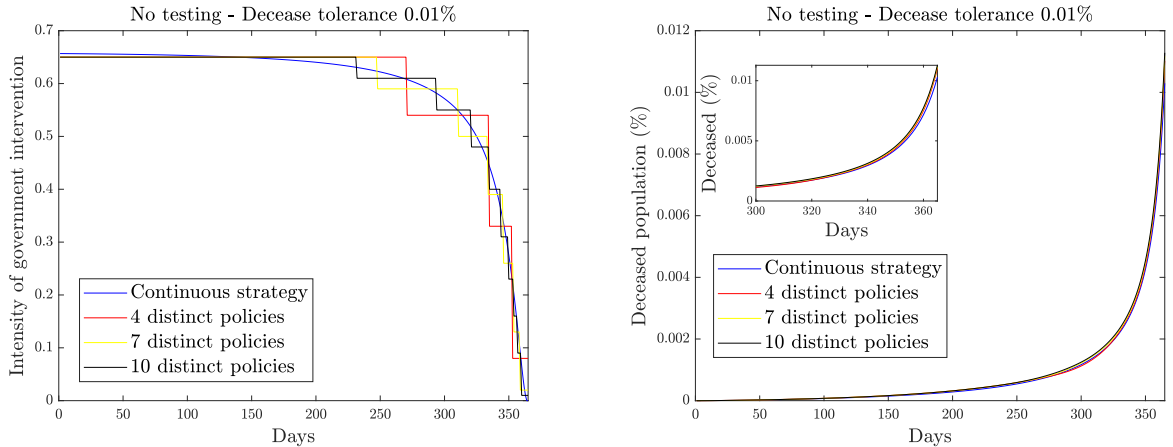


Figure 13: Intervention strategy and decrease rate, 0.01% decrease tolerance, no testing. Intensity of government intervention (left) and portion of deceased population (right) when no testing is performed and a decrease tolerance of 0.01% is adopted when (i) a continuously changing strategy is selected and (ii) discrete implementations of the selected strategy are considered, allowing 4, 7 and 10 policy levels and 6, 12 and 18 policy changes respectively.

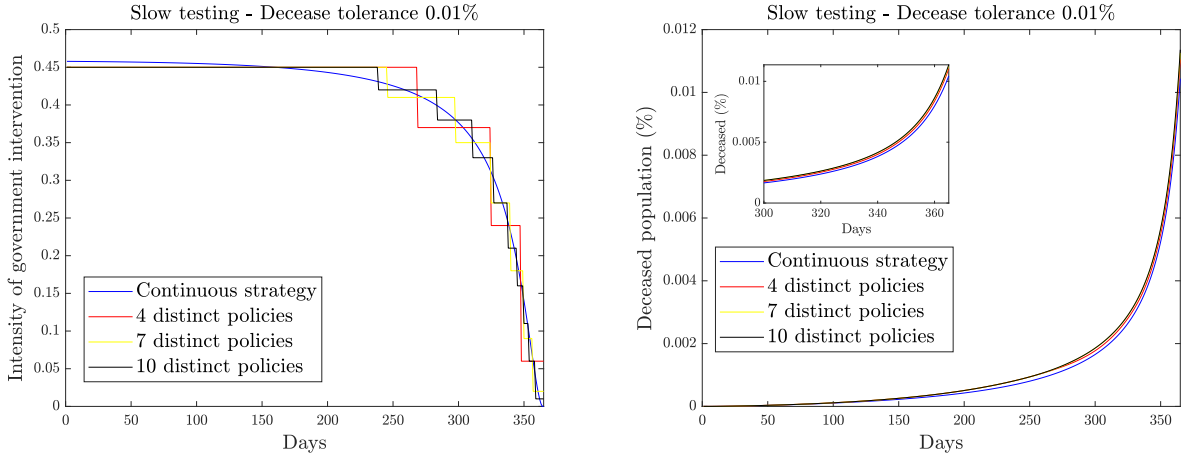


Figure 14: Intervention strategy and decrease rate, 0.01% decrease tolerance, slow testing. Intensity of government intervention (left) and portion of deceased population (right) when a slow testing policy and a decrease tolerance of 0.01% are adopted when (i) a continuously changing strategy is selected and (ii) discrete implementations of the selected strategy are considered, allowing 4, 7 and 10 policy levels and 6, 12 and 18 policy changes respectively.

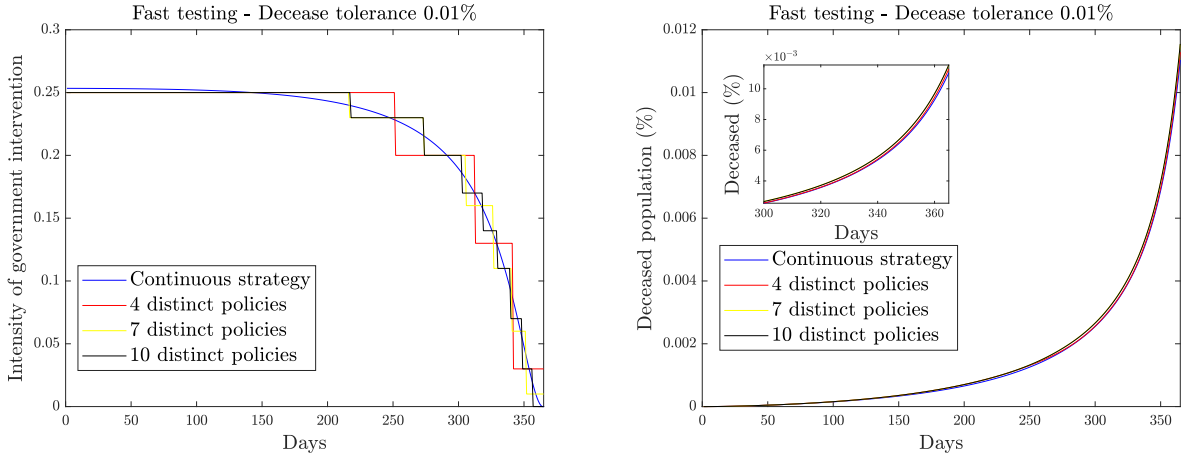


Figure 15: Intervention strategy and decrease rate, 0.01% decrease tolerance, fast testing. Intensity of government intervention (left) and portion of deceased population (right) when a fast testing policy and a decrease tolerance of 0.01% are adopted when (i) a continuously changing strategy is selected and (ii) discrete implementations of the selected strategy are considered, allowing 4, 7 and 10 policy levels and 6, 12 and 18 policy changes respectively.

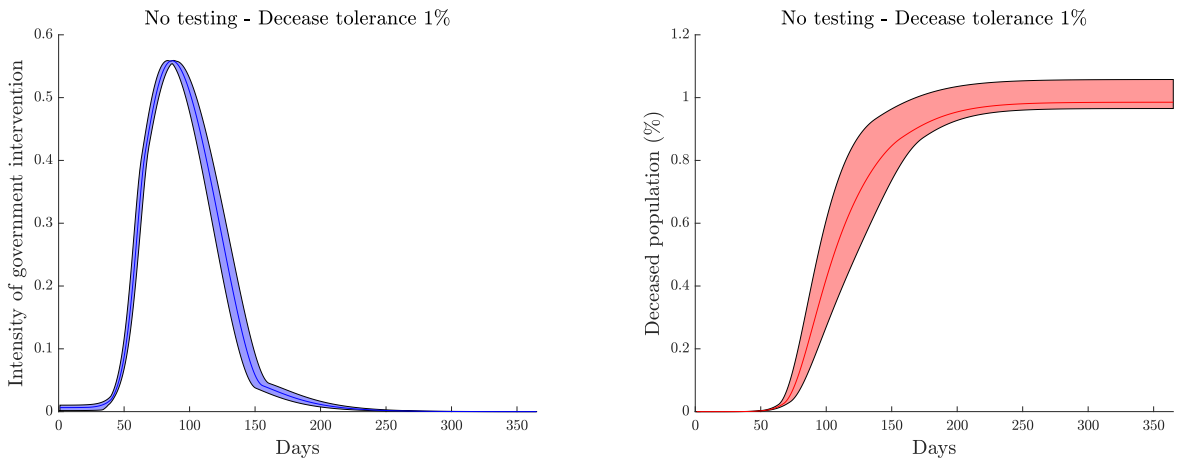


Figure 16: Effect of uncertainty in \bar{R}_0 on optimal strategy and decrease rate, 1% decrease tolerance, no testing. Both subfigures consider the range $\bar{R}_0 \in [3.17, 3.38]$, a no testing policy and a decrease tolerance of 1%. (left) Ranges of optimal strategies, (right) Ranges of aggregate decreases when the optimal strategy obtained based on $\bar{R}_0 = 3.27$ and infection mortality rate of 0.66% is implemented. The darker line within the presented ranges corresponds to $\bar{R}_0 = 3.27$.

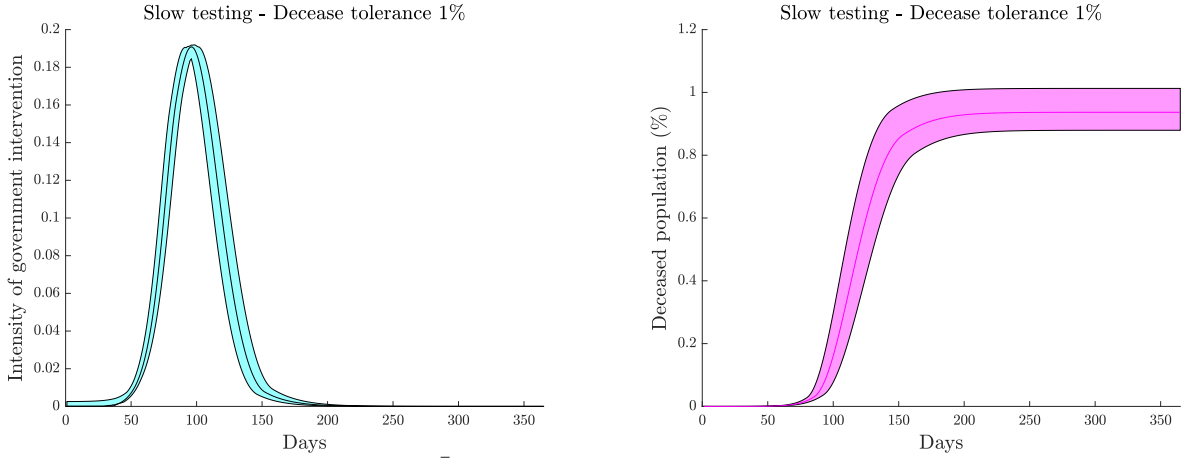


Figure 17: Effect of uncertainty in \bar{R}_0 on optimal strategy and decrease rate, 1% decrease tolerance, slow testing. Both subfigures consider the range $\bar{R}_0 \in [3.17, 3.38]$, a slow testing policy and a decrease tolerance of 1%. (left) Ranges of optimal strategies, (right) Ranges of aggregate decreases when the optimal strategy obtained based on $\bar{R}_0 = 3.27$ and infection mortality rate of 0.66% is implemented. The darker line within the presented ranges corresponds to $\bar{R}_0 = 3.27$.

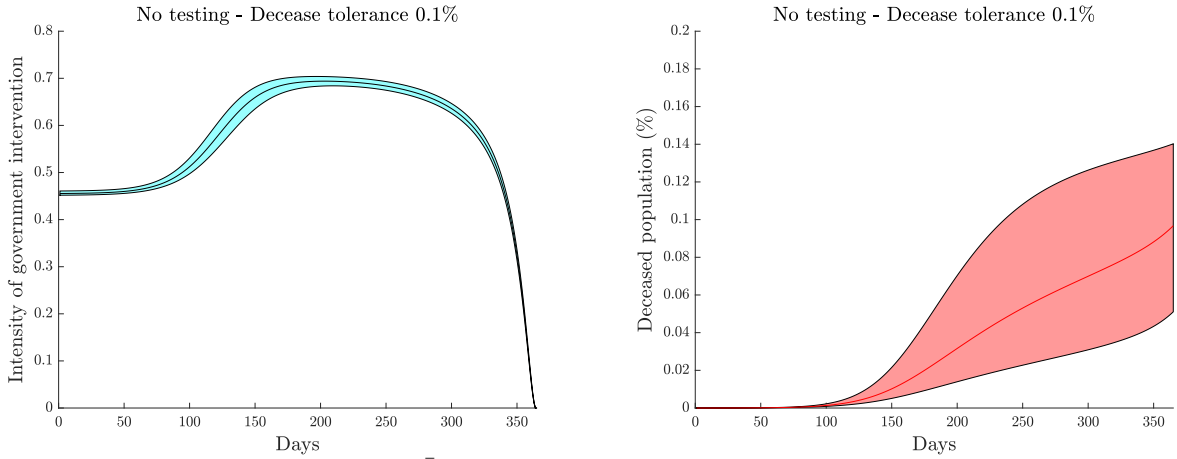


Figure 18: Effect of uncertainty in \bar{R}_0 on optimal strategy and decrease rate, 0.1% decrease tolerance, no testing. Both subfigures consider the range $\bar{R}_0 \in [3.17, 3.38]$, a no testing policy and a decrease tolerance of 0.1%. (left) Ranges of optimal strategies, (right) Ranges of aggregate decreases when the optimal strategy obtained based on $\bar{R}_0 = 3.27$ and infection mortality rate of 0.66% is implemented. The darker line within the presented ranges corresponds to $\bar{R}_0 = 3.27$.

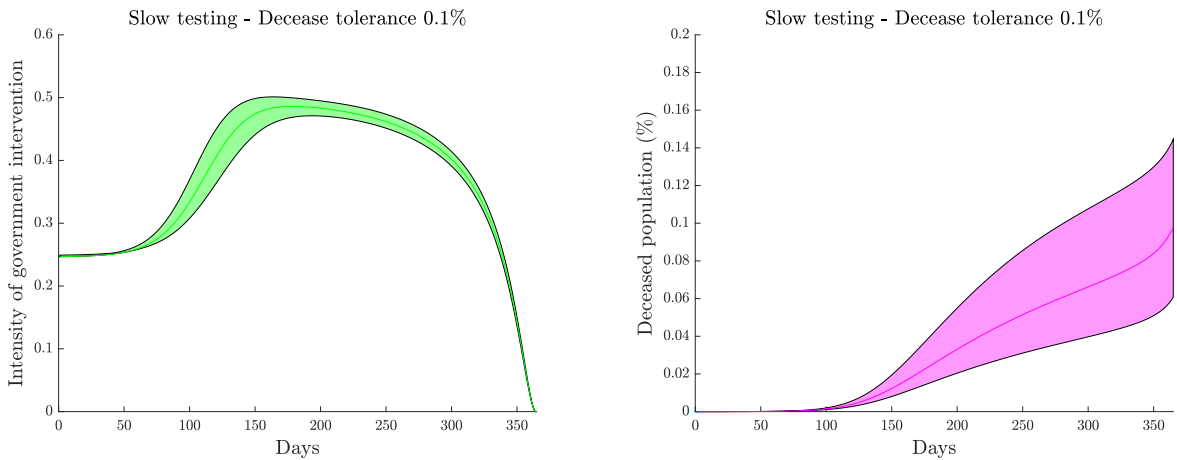


Figure 19: Effect of uncertainty in \bar{R}_0 on optimal strategy and decrease rate, 0.1% decrease tolerance, slow testing. Both subfigures consider the range $\bar{R}_0 \in [3.17, 3.38]$, a slow testing policy and a decrease tolerance of 0.1%. (left) Ranges of optimal strategies, (right) Ranges of aggregate decreases when the optimal strategy obtained based on $\bar{R}_0 = 3.27$ and infection mortality rate of 0.66% is implemented. The darker line within the presented ranges corresponds to $\bar{R}_0 = 3.27$.

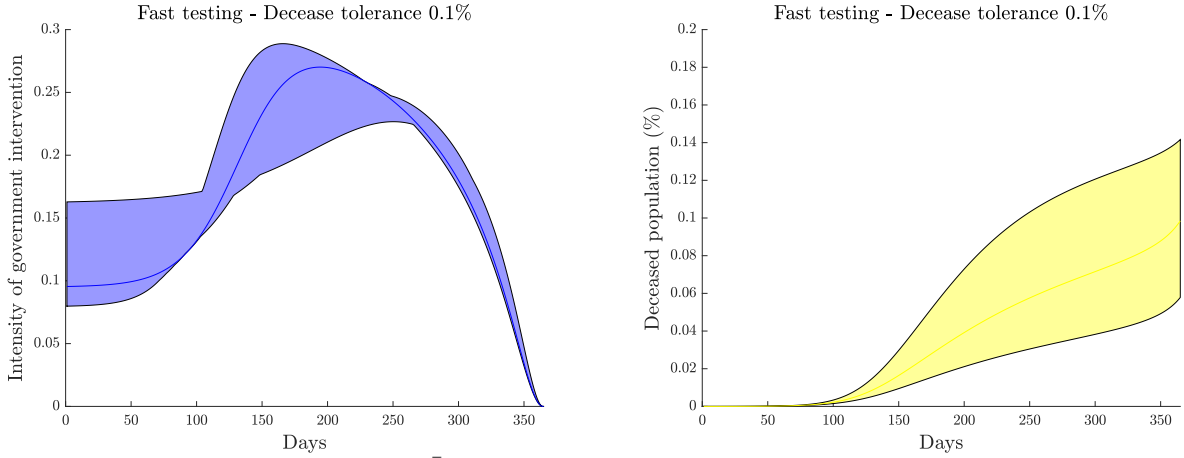


Figure 20: Effect of uncertainty in \bar{R}_0 on optimal strategy and decrease rate, 0.1% decrease tolerance, fast testing. Both subfigures consider the range $\bar{R}_0 \in [3.17, 3.38]$, a fast testing policy and a decrease tolerance of 0.1%. (left) Ranges of optimal strategies, (right) Ranges of aggregate decreases when the optimal strategy obtained based on $\bar{R}_0 = 3.27$ and infection mortality rate of 0.66% is implemented. The darker line within the presented ranges corresponds to $\bar{R}_0 = 3.27$.

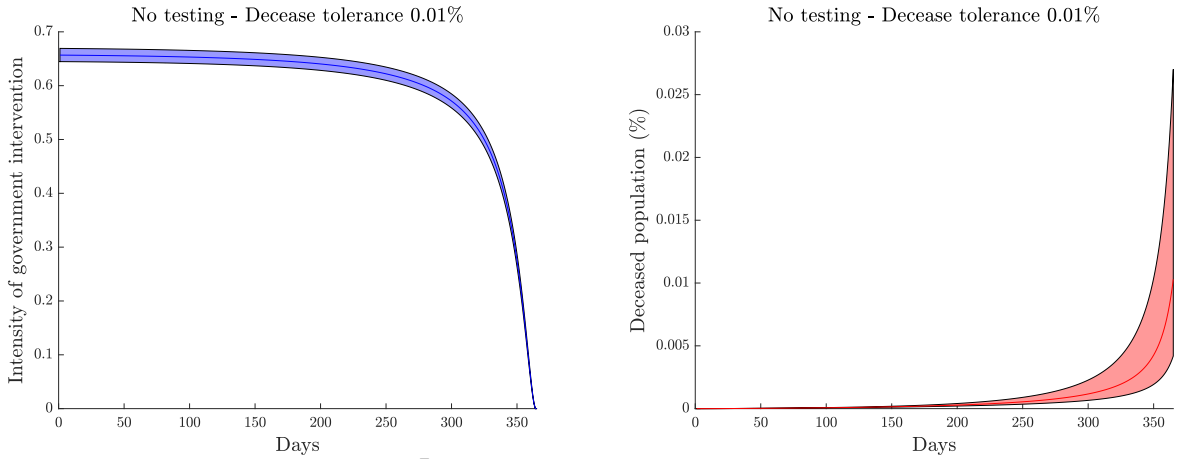


Figure 21: Effect of uncertainty in \bar{R}_0 on optimal strategy and decrease rate, 0.01% decrease tolerance, no testing. Both subfigures consider the range $\bar{R}_0 \in [3.17, 3.38]$, a no testing policy and a decrease tolerance of 0.01%. (left) Ranges of optimal strategies, (right) Ranges of aggregate decreases when the optimal strategy obtained based on $\bar{R}_0 = 3.27$ and infection mortality rate of 0.66% is implemented. The darker line within the presented ranges corresponds to $\bar{R}_0 = 3.27$.

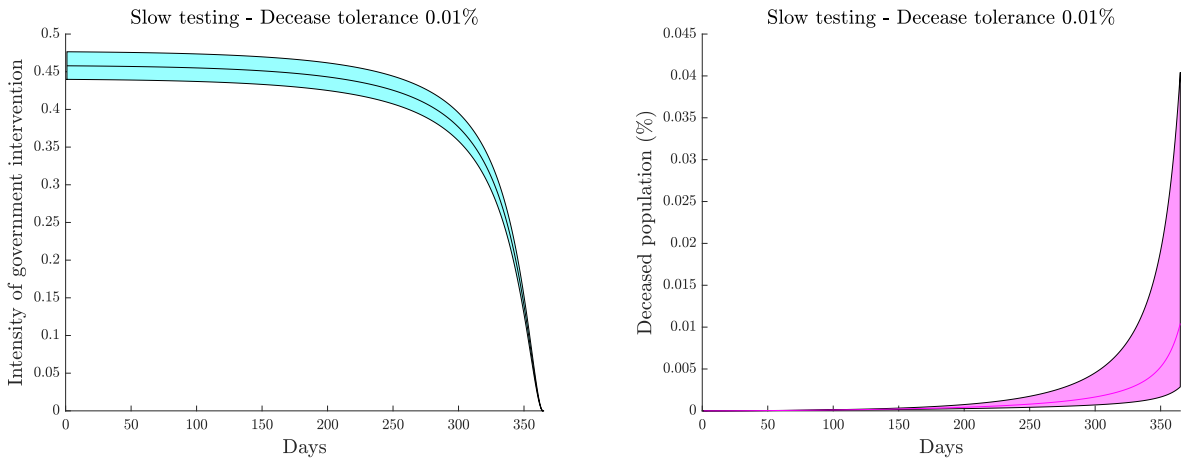


Figure 22: Effect of uncertainty in \bar{R}_0 on optimal strategy and decrease rate, 0.01% decrease tolerance, slow testing. Both subfigures consider the range $\bar{R}_0 \in [3.17, 3.38]$, a slow testing policy and a decrease tolerance of 0.01%. (left) Ranges of optimal strategies, (right) Ranges of aggregate decreases when the optimal strategy obtained based on $\bar{R}_0 = 3.27$ and infection mortality rate of 0.66% is implemented. The darker line corresponds to $\bar{R}_0 = 3.27$.

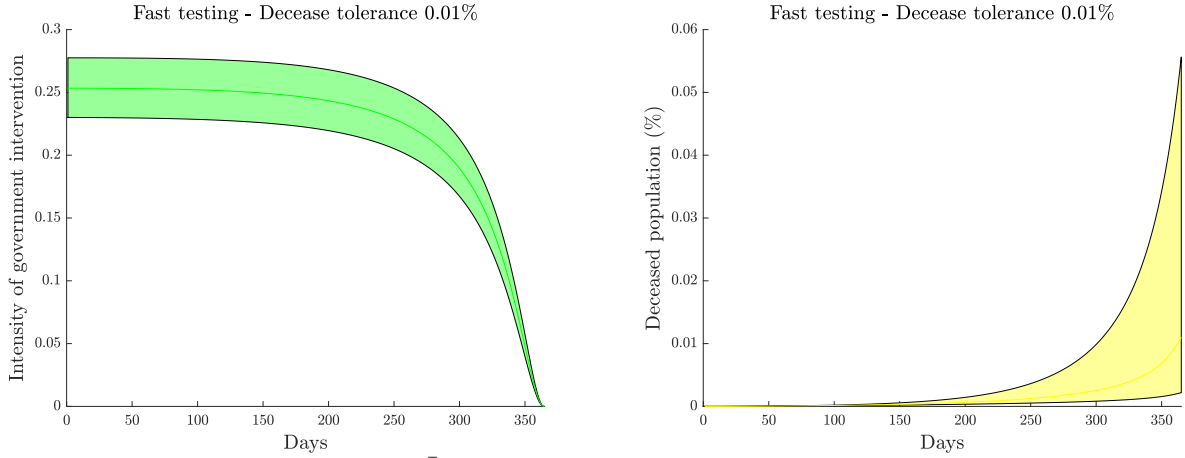


Figure 23: Effect of uncertainty in \bar{R}_0 on optimal strategy and decrease rate, 0.01% decrease tolerance, fast testing. Both subfigures consider the range $\bar{R}_0 \in [3.17, 3.38]$, a fast testing policy and a decrease tolerance of 0.01%. (left) Ranges of optimal strategies, (right) Ranges of aggregate decreases when the optimal strategy obtained based on $\bar{R}_0 = 3.27$ and infection mortality rate of 0.66% is implemented. The darker line corresponds to $\bar{R}_0 = 3.27$.

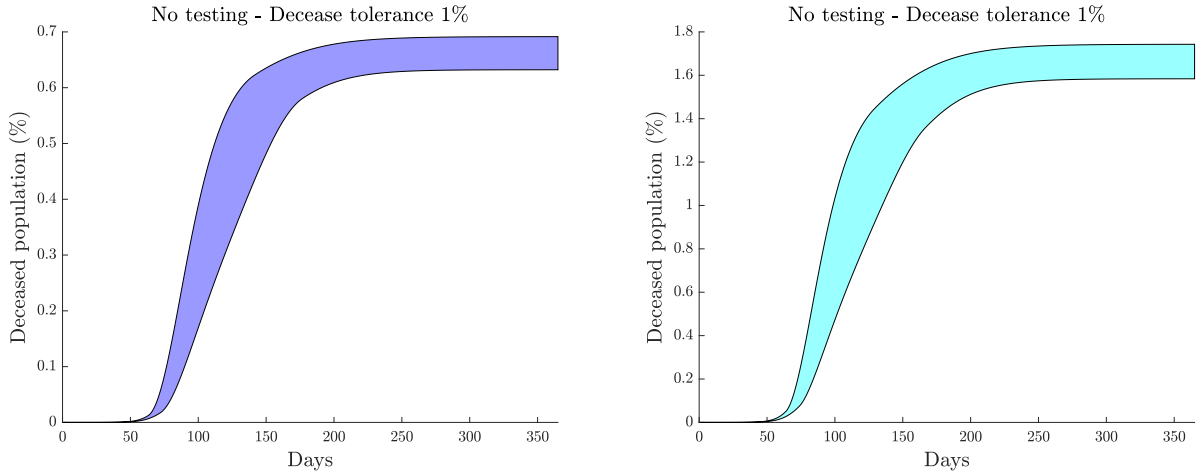


Figure 24: Combined effect of uncertainty in \bar{R}_0 and infection fatality rate on the decrease rate, 1% decrease tolerance, no testing. Ranges of aggregate decreases for $\bar{R}_0 \in [3.17, 3.38]$ when no testing is performed and a decrease tolerance of 1% is adopted with infection mortality rates of 0.39% (left) and 1.33% (right) when the optimal strategy obtained based on $\bar{R}_0 = 3.27$ and infection mortality rate of 0.66% is implemented.

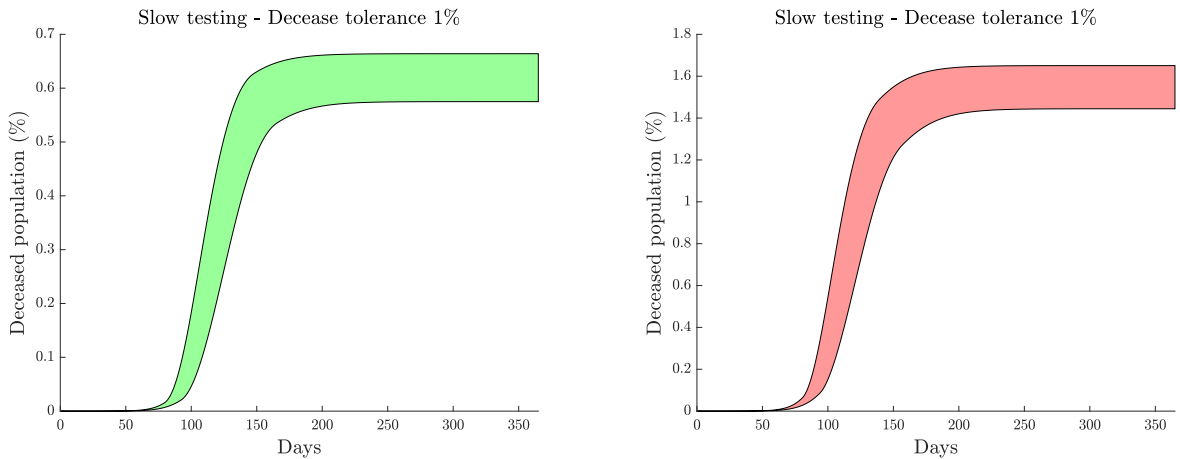


Figure 25: Combined effect of uncertainty in \bar{R}_0 and infection fatality rate on the decrease rate, 1% decrease tolerance, slow testing. Ranges of aggregate decreases for $\bar{R}_0 \in [3.17, 3.38]$ when a slow testing policy and a decrease tolerance of 1% are adopted with infection mortality rates of 0.39% (left) and 1.33% (right) when the optimal strategy obtained based on $\bar{R}_0 = 3.27$ and infection mortality rate of 0.66% is implemented.

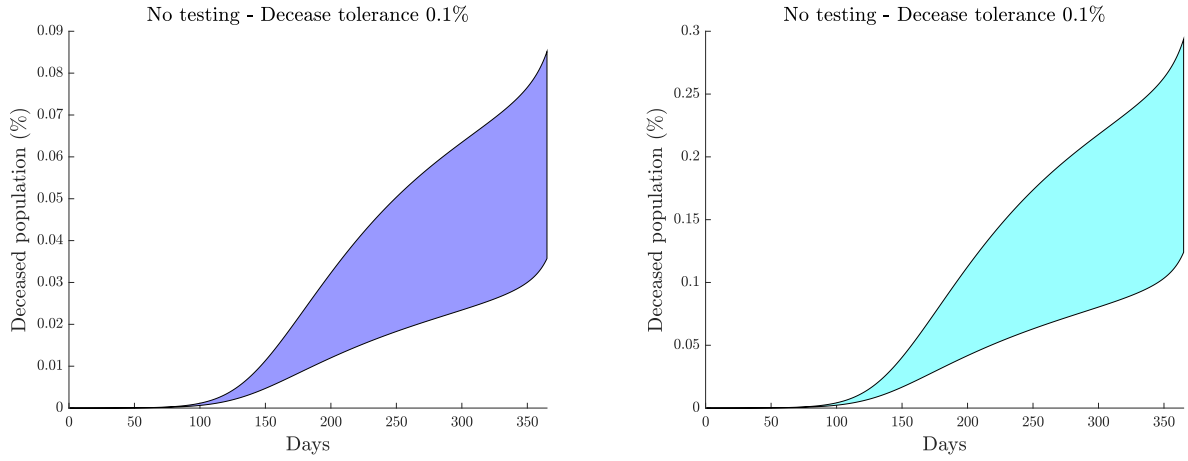


Figure 26: Combined effect of uncertainty in \bar{R}_0 and infection fatality rate on the decease rate, 0.1% decease tolerance, no testing. Ranges of aggregate deceases for $\bar{R}_0 \in [3.17, 3.38]$ when no testing is performed and a decease tolerance of 0.1% is adopted with infection mortality rates of 0.39% (left) and 1.33% (right) when the optimal strategy obtained based on $\bar{R}_0 = 3.27$ and infection mortality rate of 0.66% is implemented.

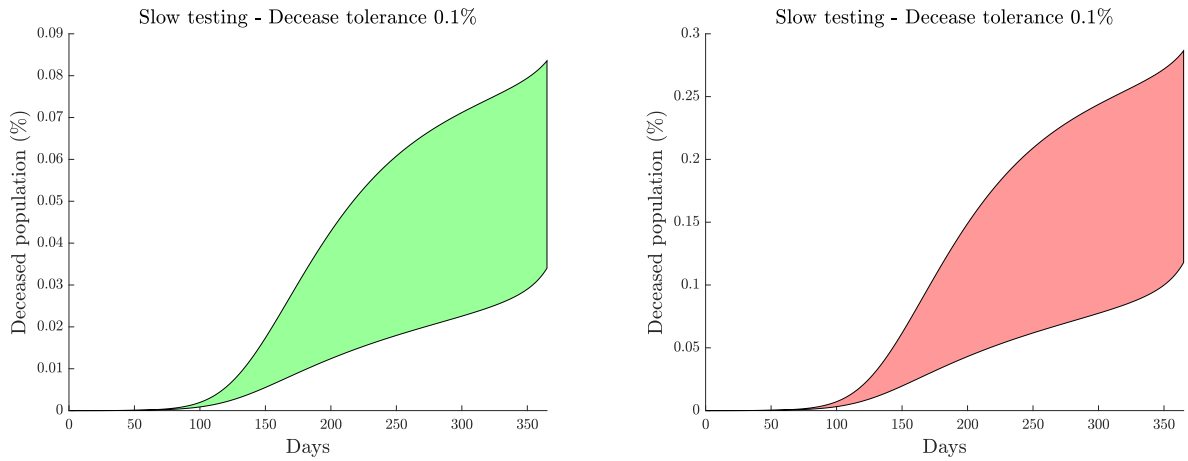


Figure 27: Combined effect of uncertainty in \bar{R}_0 and infection fatality rate on the decease rate, 0.1% decease tolerance, slow testing. Ranges of aggregate deceases for $\bar{R}_0 \in [3.17, 3.38]$ when a slow testing policy and a decease tolerance of 0.1% are adopted with infection mortality rates of 0.39% (left) and 1.33% (right) when the optimal strategy obtained based on $\bar{R}_0 = 3.27$ and infection mortality rate of 0.66% is implemented.

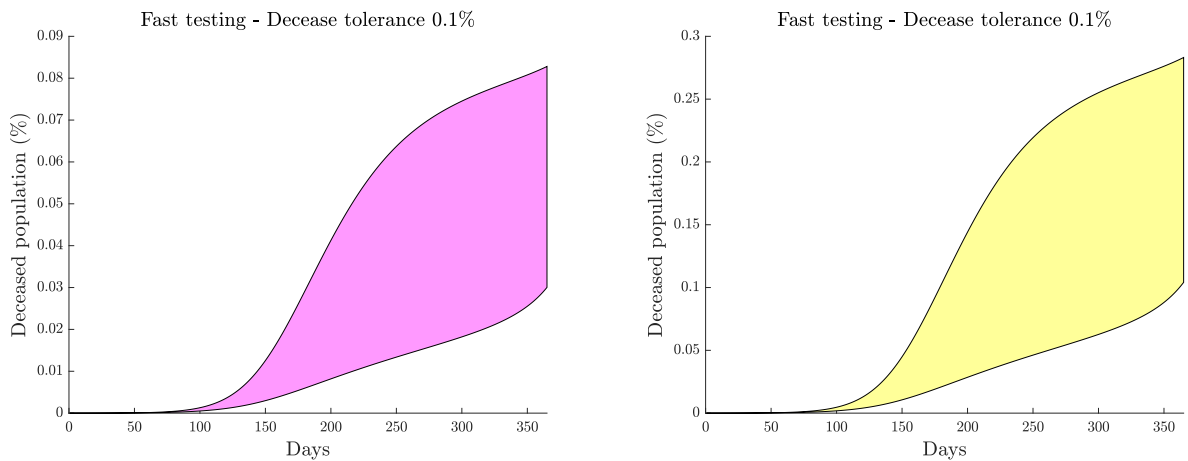


Figure 28: Combined effect of uncertainty in \bar{R}_0 and infection fatality rate on the decease rate, 0.1% decease tolerance, fast testing. Ranges of aggregate deceases for $\bar{R}_0 \in [3.17, 3.38]$ when a fast testing policy and a decease tolerance of 0.1% are adopted with infection mortality rates of 0.39% (left) and 1.33% (right) when the optimal strategy obtained based on $\bar{R}_0 = 3.27$ and infection mortality rate of 0.66% is implemented.

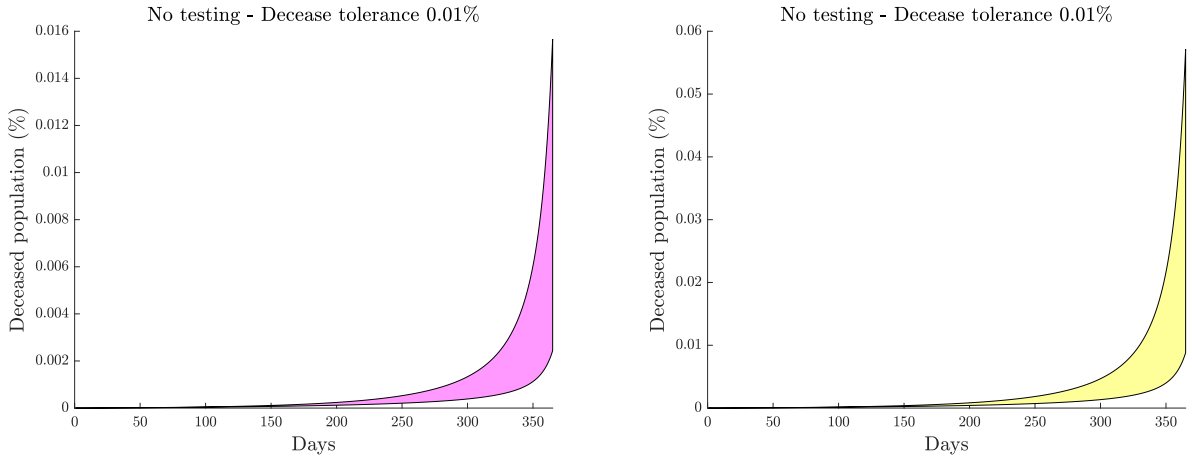


Figure 29: Combined effect of uncertainty in \bar{R}_0 and infection fatality rate on the decease rate, 0.01% decease tolerance, no testing. Ranges of aggregate deceases for $\bar{R}_0 \in [3.17, 3.38]$ when no testing is performed and a decease tolerance of 0.01% is adopted with infection mortality rates of 0.39% (left) and 1.33% (right) when the optimal strategy obtained based on $\bar{R}_0 = 3.27$ and infection mortality rate of 0.66% is implemented.

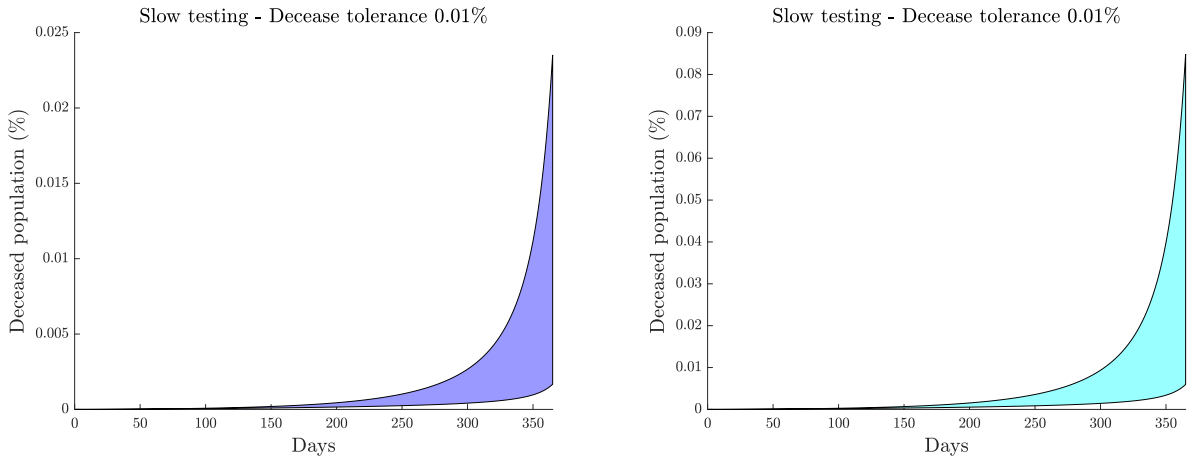


Figure 30: Combined effect of uncertainty in \bar{R}_0 and infection fatality rate on the decease rate, 0.01% decease tolerance, slow testing. Ranges of aggregate deceases for $\bar{R}_0 \in [3.17, 3.38]$ when a slow testing policy and a decease tolerance of 0.01% are adopted with infection mortality rates of 0.39% (left) and 1.33% (right) when the optimal strategy obtained based on $\bar{R}_0 = 3.27$ and infection mortality rate of 0.66% is implemented.

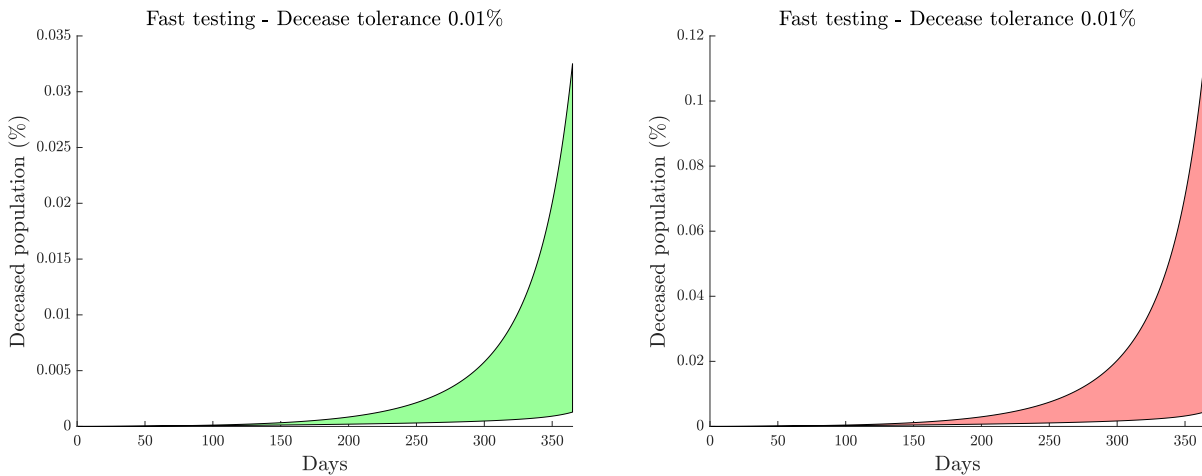


Figure 31: Combined effect of uncertainty in \bar{R}_0 and infection fatality rate on the decease rate, 0.01% decease tolerance, fast testing. Ranges of aggregate deceases for $\bar{R}_0 \in [3.17, 3.38]$ when a fast testing policy and a decease tolerance of 0.01% are adopted with infection mortality rates of 0.39% (left) and 1.33% (right) when the optimal strategy obtained based on $\bar{R}_0 = 3.27$ and infection mortality rate of 0.66% is implemented.

References

- [1] Li, R. *et al.* Substantial undocumented infection facilitates the rapid dissemination of novel coronavirus (SARS-CoV-2). *Science* **368**, 489–493 (2020).
- [2] International Coronaviridae Study Group. *et al.* The species severe acute respiratory syndrome-related coronavirus: classifying 2019-ncov and naming it SARS-CoV-2. *Nature Microbiology* **5**, 536 (2020).
- [3] Maier, B. F. & Brockmann, D. Effective containment explains subexponential growth in recent confirmed COVID-19 cases in China. *Science* **368**, 742–746 (2020).
- [4] Maharaaj, S. & Kleczkowski, A. Controlling epidemic spread by social distancing: Do it well or not at all. *BMC Public Health* **12**, 679 (2012).
- [5] International Monetary Fund. World economic outlook: Gross domestic product (October 2020).
- [6] Kermack, W. O. & McKendrick, A. G. A contribution to the mathematical theory of epidemics. *Proceedings of the royal society of london. Series A, Containing papers of a mathematical and physical character* **115**, 700–721 (1927).
- [7] Hethcote, H. W. The mathematics of infectious diseases. *SIAM review* **42**, 599–653 (2000).
- [8] Dehning, J. *et al.* Inferring COVID-19 spreading rates and potential change points for case number forecasts. *Preprint at <https://arxiv.org/abs/2004.01105>* (2020).
German, R., Djanatliev, A., Maile, L., Bazan, P. & Hackstein, H. Modeling exit strategies from COVID-19 lockdown with a focus on antibody tests. *medRxiv* (2020).
- [9] Giordano, G. *et al.* Modelling the COVID-19 epidemic and implementation of population-wide interventions in italy. *Nature Medicine* 1–6 (2020).
- [10] Della Rossa, F. *et al.* A network model of italy shows that intermittent regional strategies can alleviate the covid-19 epidemic. *Nature communications* **11**, 1–9 (2020).
- [11] Alimohamadi, Y., Taghdir, M. & Sepandi, M. The estimate of the basic reproduction number for novel coronavirus disease (COVID-19): a systematic review and meta-analysis. *Journal of Preventive Medicine and Public Health* (2020).
- [12] Yuan, J., Li, M., Lv, G. & Lu, Z. K. Monitoring transmissibility and mortality of COVID-19 in europe. *International Journal of Infectious Diseases* (2020).
- [13] Gatto, M. *et al.* Spread and dynamics of the covid-19 epidemic in italy: Effects of emergency containment measures. *Proceedings of the National Academy of Sciences* **117**, 10484–10491 (2020).
- [14] Verity, R., *et al.* Estimates of the severity of coronavirus disease 2019: a model-based analysis. *The Lancet infectious diseases* (2020).
- [15] Mallapaty, S. How deadly is the coronavirus? scientists are close to an answer. *Nature* **582**, 467–468 (2020).
- [16] Salje, H. *et al.* Estimating the burden of SARS-CoV-2 in france. *Science* (2020).
- [17] Flaxman, S. *et al.* Estimating the effects of non-pharmaceutical interventions on COVID-19 in europe. *Nature* (2020).
- [18] Djidjou-Demasse, R., Michalakis, Y., Choisy, M., Sofonea, M. T. & Alizon, S. Optimal COVID-19 epidemic control until vaccine deployment. *Preprint at <https://www.medrxiv.org/content/10.1101/2020.04.02.20049189v3>* (2020).
- [19] Rowthorn, R. & Maciejowski, J. A cost–benefit analysis of the COVID-19 disease. *Oxford Review of Economic Policy* **36**, S38–S55 (2020).
- [20] Köhler, J. *et al.* Robust and optimal predictive control of the COVID-19 outbreak. *Preprint at <https://arxiv.org/abs/2005.03580>* (2020).
- [21] Tsay, C., Lejarza, F., Stadtherr, M. A. & Baldea, M. Modeling, state estimation, and optimal control for the US COVID-19 outbreak. *Preprint at <https://arxiv.org/abs/2004.06291>* (2020).

- [22] Bin, M. *et al.* On fast multi-shot epidemic interventions for post lock-down mitigation: Implications for simple COVID-19 models. *Preprint at <https://arxiv.org/abs/2003.09930>* (2020).
- [23] Alvarez, F. E., Argente, D. & Lippi, F. A simple planning problem for COVID-19 lockdown. Tech. Rep., National Bureau of Economic Research (2020).
- [24] Acemoglu, D., Chernozhukov, V., Werning, I. & Whinston, M. D. Optimal targeted lockdowns in a multi-group sir model. *NBER Working Paper No 27102* (2020).
- [25] World Health Organization. Report of the WHO - China joint mission on coronavirus disease 2019 (COVID-19) (2020).
- [26] Wang, H. *et al.* Phase-adjusted estimation of the number of coronavirus disease 2019 cases in wuhan, China. *Cell discovery* **6**, 1–8 (2020).
- [27] United Nations, Department of Economic and Social Affairs. Population data (Retrieved on 30/11/2020). <https://population.un.org/wpp/DataQuery/>. United Nations, Department of Economic and Social Affairs, Retrieved on 30/11/2020.
- [28] Rhodes, A., Ferdinande, P., Flaatten, H., Guidet, B., Metnitz, P. G. & Moreno, R. P. The variability of critical care bed numbers in europe. *Intensive care medicine* **38**, 1647–1653 (2012).
- [29] Catena, R. & Holweg, M. We need to relocate ICU patients out of COVID-19 hotspots. *Harvard Business Review* (2020).
- [30] Khalil, H. K. *Nonlinear systems*, vol. 3 (Prentice Hall New Jersey, 1996).
- [31] Haddad, W. M. & Chellaboina, V. *Nonlinear dynamical systems and control: a Lyapunov-based approach* (Princeton university press, 2011).
- [32] Fleming, W. H. & Rishel, R. W. *Deterministic and stochastic optimal control*, vol. 1 (Springer Science & Business Media, 2012).
- [33] Pontryagin, L. S. *Mathematical theory of optimal processes* (Routledge, 2018).
- [34] Rockafellar, R. T. *Convex analysis* (Princeton university press, 2015).
- [35] Filippov, A. *Differential Equations with Discontinuous Righthand Sides: Control Systems*, vol. 18 (Springer Science & Business Media, 1988).
- [36] Lenhart, S. & Workman, J. T. *Optimal control applied to biological models* (CRC press, 2007).
- [37] Abbott, S. *Understanding analysis*, vol. 2 (Springer, 2001).
- [38] Hallal, P. *et al.* Remarkable variability in SARS-CoV-2 antibodies across brazilian regions: nationwide serological household survey in 27 states. *medRxiv* (2020).

Acknowledgements

This work was funded by the European Union’s Horizon 2020 research and innovation program under grant agreement 739551 (KIOS CoE) and from the Republic of Cyprus through the Directorate General for European Programs, Coordination, and Development.